AD-A172 801 AFGWC'S ADVANCED WEATHER ANALYSIS AND PREDICTION SYSTEM 1/1
(AWAPS)(U) AIR COMMAND AND STAFF COLL MAXWELL AFB AL
J G STOBIE JUN 86 ACSC-86-2405 AWS-TN-86/001

UNCLASSIFIED F/G 4/2 NL

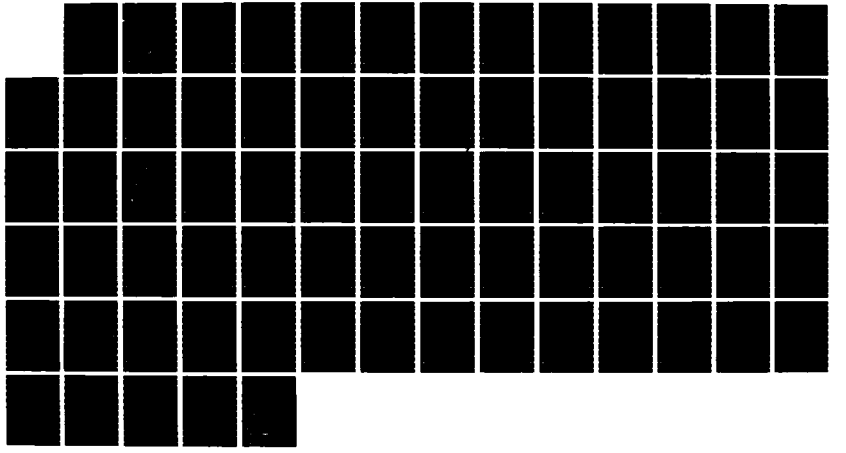

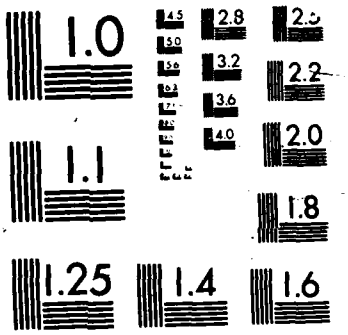
1.0
1.1
1.25
1.4
1.6
1.8
2.0
2.2
2.8
3.2
3.6
4.0

(2)

AWS/TN-86/001

AD-A172 801

AFGWC's

ADVANCED WEATHER ANALYSIS

AND

PREDICTION SYSTEM

(AWAPS)

By

JAMES G. STOBIE, Major, USAF

JUNE 1986

AIR WEATHER SERVICE (MAC)

Scott Air Force Base, Illinois, 62225-5008

REVIEW AND APPROVAL STATEMENT

This publication approved for public release. There is no objection to unlimited distribution of the document to the public at large, or by the Defense Technical Information Center (DTIC) to the National Technical Information Service (NTIS).

This technical publication has been reviewed and is approved for publication.

CLIFFORD R. MATSUMOTO, Major, USAF

FOR THE COMMANDER

JOHN W. OLIVER, Colonel, USAF
Asst DCS/Aerospace Sciences

UNCLASSIFIED

REPORT DOCUMENTATION PAGE

1a. Report Security Classification: UNCLASSIFIED

3. Distribution/Availability of Report: Approved for public release; distribution unlimited.

4. Performing Organization Report Number: ACSC 86-2405

5. Monitoring Organization Report Number: AWS/TN-86/001

6a. Name of Performing Organization: Air Command and Staff College 6b. Office Symbol: EDCC

6c. Address: Maxwell AFB, AL 36112-5542

7a. Name of Monitoring Organization: Air Weather Service (AWS/DN)

7b. Address: Scott AFB, IL 62225-5438

11. Title: AFGWC's Advanced Weather Analysis and Prediction System (AWAPS) (Unclassified)

12. Personal Author: James G. Stobie, Major, USAF

13a. Type of Report: Technical Note 14. Date of Report: June 1986 15. Page Count: 68

16. Supplementary Notation: Adapted from Air Command and Staff Research Report 86-2405; reprinted with ACSC permission.

17. COSATI Codes: *Field--04, Group--02*

18. Subject Terms: *METEOROLOGY, *COMPUTERS, COMPUTER ARCHITECTURE, COMPUTER MODELS, COMPUTER APPLICATIONS, WEATHER FORECASTING, WEATHER ANALYSIS, *NUMERICAL WEATHER PREDICTION, MILITARY METEOROLOGY.

19. Abstract: Describes the three computer models used in the Air Force Global Weather Central's Advanced Weather Analysis and Prediction System (AWAPS) and explains how they interact to form a production cycle. These models are the High Resolution Analysis System (HIRAS), the Global Spectral Model (GSM), and the Relocatable Window Model (RWM). Also gives a brief introduction to the basics of numerical weather prediction.

20. Distribution/Availability of Abstract: Same as report

21. Abstract Security Classification: UNCLASSIFIED

22a. Name of Responsible Individual: Kenneth D. Hill

22b. Telephone: 618 256-4741

22c. Office Symbol: AWS/DNT

DD FORM 1473

UNCLASSIFIED

PREFACE

On 23 October 1985, the Air Weather Service (AWS) entered a new era in weather forecasting. On that date, the Air Force Global Weather Central (AFGWC) implemented its new Advanced Weather Analysis and Prediction System (AWAPS). By December 1985, AFGWC's aviation wind forecasts had improved by 20 percent, and AWAPS continues to provide vastly improved weather forecasts to AWS units around the world.

Actually, AWAPS is more than just forecasts. It is a massive computer hardware and software system. The heart of the AWAPS is a Cray X-MP supercomputer, the fastest in the Department of Defense inventory. Running on the Cray X-MP are three numerical weather prediction (NWP) models: The High Resolution Analysis System (HIRAS), the Global Spectral Model, (GSM), and the Relocatable Window Model (RWM). The HIRAS is a global analysis system that blends conventional, aircraft, and satellite observations into a single, concise weather analysis. The GSM is a state-of-the-art forecast model that forecasts the weather for the entire world. The RWM is a regional scale model, tailor-made for contingency operations anywhere in the world.

This report examines the software portion of the AWAPS. It gives a brief description of the three AWAPS models, paying particualar attention to the individual strengths and weaknesses of each, and describes how the AWAPS models interact to form a production cycle. It aso provides some basic NWP principles. The main objective of the report is to give AWS forecasters an idea of how the AWAPS works and help them get the most out of AWAPS products.

This document was written as a student research project (ACSC 86-2405) at the Air Command and Staff College, Maxwell AFB, Alabama, and has been adapted and reprinted with permission. The author would like to thank those people who assisted in the basic research and who provided helpful guidance by reviewing the manuscript. They are Lt Col Dennis Bieliicki, Lt Col Jim Koermer, Lt Col Doug Moore, Lt Col Roger Whiton, Maj Herm Fresh, Maj Jack Hayes, Maj Cliff Matsumoto, Maj Dan White, Capt Carol Belt, Capt Jason Tuell, and Mr Ed Carr.

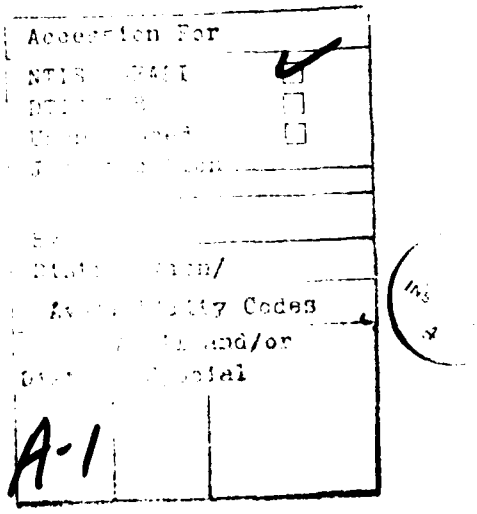

TABLE OF CONTENTS

DEFINITIONS

AFGWC	Air Force Global Weather Central
AWAPS	Advanced Weather Analysis and Prediction System
AWS	Air Weather Service
AWSPE	Air Weather Service Primitive Equation model
BOGUS	Artificial observations created by AFGWC forecasters
GSM	Global Spectral Model
HIRAS	High Resolution Analysis System
LFM	Limited area Fine Mesh forecast model (NMC)
MFM	Movable Fine Mesh model (NMC)
OI	Optimum Interpolation
NMC	National Meteorological Center
NMI	Normal Mode Initialization
NWP	Numerical Weather Prediction
PE	Primitive Equation model (NMC)
QC	Quality Control
RAOB	Radiosonde Observation
RH	Relative Humidity
RMS	Root Mean Square
RWM	Relocatable Window Model
SFC	Surface
WMO	World Meteorological Organization

LIST OF ILLUSTRATIONS

Chapter 1 - Introduction

The purpose of this report is to help you get the most out of the Air Force Global Weather Central's (AFGWC) advanced weather analysis and prediction system (AWAPS).

If you're an AWS forecaster, you're probably already using AWAPS products. That's because AWAPS produces nearly all of AFGWC's automated forecasts, with the exception of clouds. These forecasts feed computer flight plans, facsimile charts, and teletype bulletins. Furthermore, the AWAPS models provide important input for AFGWC's cloud models.

Installed in 1985, the AWAPS represents a giant step forward in numerical weather prediction (NWP) at AFGWC. The AWAPS includes three state-of-the-art models: the high resolution analysis system (HIRAS), the global spectral model (GSM), and the relocatable window model (RWM). These models run on a Cray X-MP supercomputer, the fastest computer in the Department of Defense inventory.

To really get the most out of AWAPS you need to know both its strengths and weaknesses. You need to know when to trust it and when not to trust it; that's what this report is all about.

This report is divided into seven chapters. Chapter 2 looks at some NWP basics. Specifically, it defines some of the NWP terms used in the remaining chapters. Chapter 3 examines how the three AWAPS models fit together into a production cycle. Unlike the old AFGWC analysis/forecast system, the AWAPS production cycle is really quite simple. In Chapter 4 we get into the models themselves, in this case, the HIRAS. But, we stay away from the theory and concentrate on those things that really pertain to you, the forecaster. Chapter 5 looks at the GSM. Since the GSM has over four years of operational history at the National Meteorological Center (NMC), it already has some well-established rules of thumb. This chapter lists some of those rules along with some of the GSM's unique characteristics. Chapter 6 takes a very quick look at the RWM. The reason we don't spend much time on the RWM is because it really has no operational history. In fact, it has not even been implemented on the AWAPS yet. Finally, Chapter 7 wraps things up with a brief summary and conclusion.

Chapter 2 - Basics of Numerical Weather Prediction (NWP)

A. General

To understand some of the basic NWP principles behind the three AWAPS models, let's consider a very simple case. This case illustrates two important points: (1) the difference between an analysis model and a forecast model, and (2) the difference between a grid-point model and a spectral model.

B. Numerical Analysis

Fig. 2-1 shows a hypothetical temperature field valid at 00Z. Notice that for this very special case the isotherms are a series of straight, parallel lines.

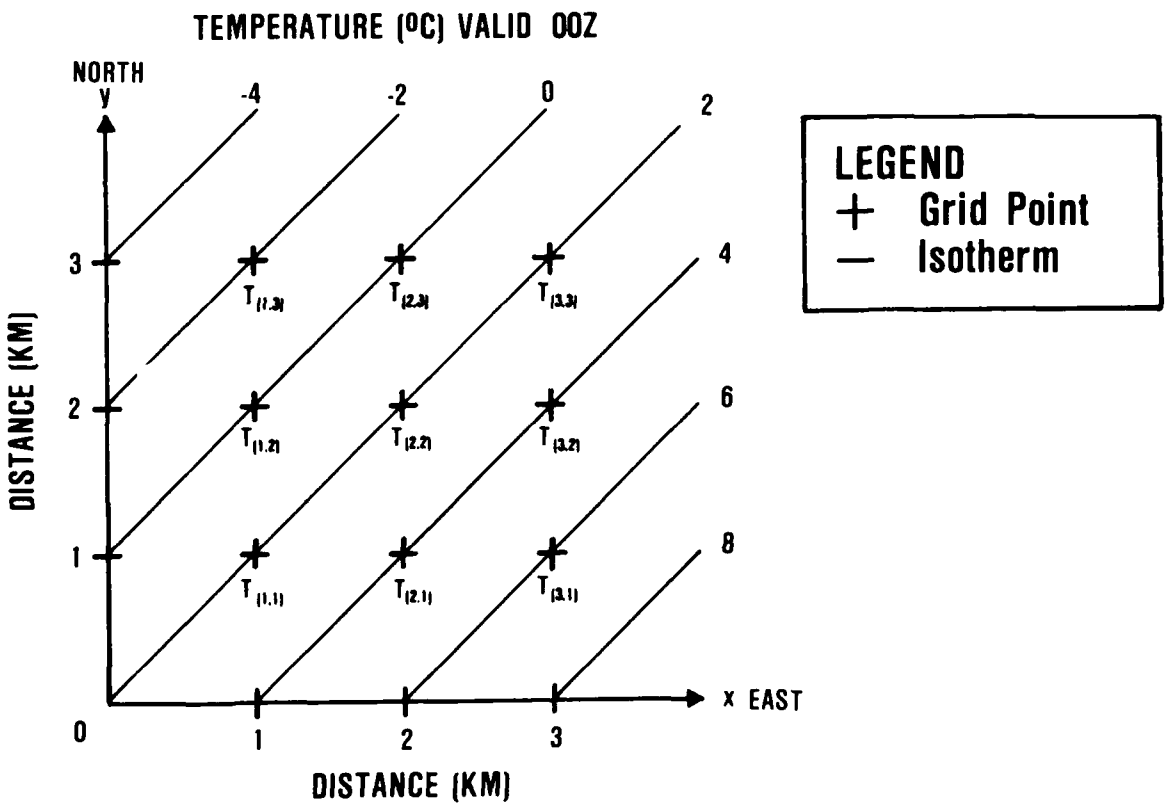

Fig. 2-1. Hypothetical temperature field and a 9-point grid.

1. Grid-Point Method

The first step in any model is to convert the observed field into a form that the computer can understand. One way to do this is to approximate the field as a series of points. For example, we could approximate the temperature field in Fig. 2-1 by the nine points labeled T(x,y). We would simply tell the computer what the temperature is at each of these points. Here is how the computer would actually receive this information:

T(1,1) = 2
T(2,1) = 4
T(3,1) = 6
T(1,2) = 0
T(2,2) = 2
T(3,2) = 4
T(1,3) = -2
T(2,3) = 0
T(3,3) = 2.*

This is called a grid-point analysis.

2. Spectral Method

Another way to represent this field would be as an equation. In this case, the equation of a plane fits best. This equation would be

$$T(x,y) = 2 + 2x - 2y. \qquad (1)$$

This type of representation is analogous to a spectral representation.** Note also, that if you plug in the appropriate values for x and y, you can still obtain the grid-point values.

3. Other Analysis Fields

Temperature is not the only field that can be represented by these two methods. In fact, before we can make a forecast, we'll need one more analysis field, specifically, wind. Typically, we break the wind into two components, using U to represent the westerly component and V to represent the southerly component.

For this simple example, let's assume that there is no southerly wind component and that all the winds are blowing out of the west as shown in Fig. 2-2. Furthermore, to simplify future calculations, let's measure the wind in

---

* In this notation the numbers inside the parentheses are the x,y coordinates of the particular point. For example, T(1,2) is the temperature at the point x=1, y=2.

** A true spectral representation uses an equation that combines sines and cosines. However, for the purpose of this illustration, consider the equation of a plane to also be a form of spectral representation.

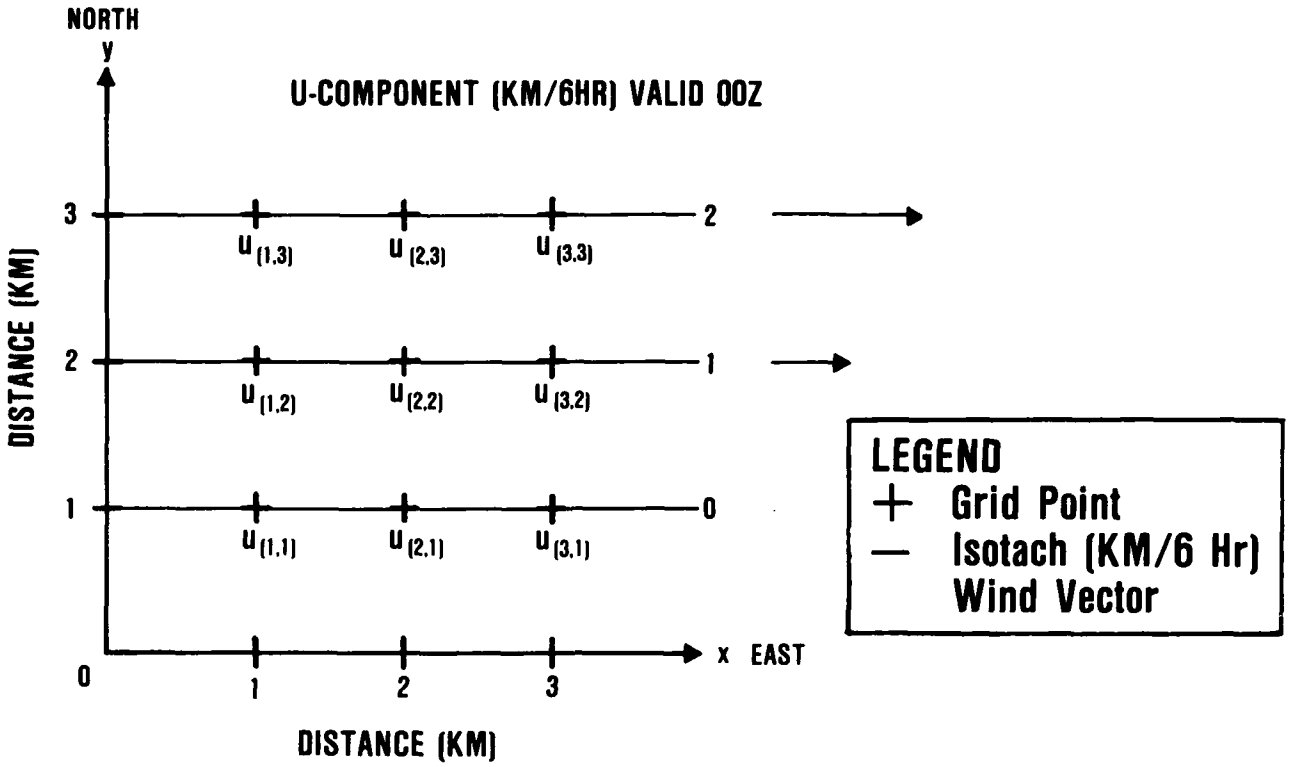

Fig. 2-2. Hypothetical u-component wind field and a 9-point grid.

km/6 hr. Using these units, the grid-point representation of the winds in Fig. 2-2 is

$$U(1,1) = 0$$
$$U(2,1) = 0$$
$$U(3,1) = 0$$
$$U(1,2) = 1$$
$$U(2,2) = 1$$
$$U(3,2) = 1$$
$$U(1,3) = 2$$
$$U(2,3) = 2$$
$$U(3,3) = 2$$

and the spectral representation

$$U(x,y) = y - 1. \qquad (2)$$

C. Numerical Forecasts

Once these fields are in either grid-point or spectral form, the computer can use equations based on the laws of physics to produce a forecast. For this example, assume that the temperature field is simply advected by the wind field.

1. Grid-Point Method

To see how a grid-point forecast works, let's first look at the middle grid point in Figs. 2-1 and 2-2. At this point

$$T(2,2) = 2^{\circ}C$$

and

$$U(2,2)=1/6 \text{ km/hr.}$$

Also notice that the temperature gradient parallel to the wind is 2°C/km. Since the wind is blowing from lower to higher temperature, it is advecting cold air. Therefore, the temperature T(2,2) at any time t will be

$$T(2,2,t) = 2^{\circ}C - (2^{\circ}C/km)(1/6 \text{ km/hr})t$$

or

$$= 2 - (2/6)t$$

where T is in °C and t is in hours. In other words, the forecast temperature is the present temperature, 2, plus the rate of temperature advection, (2/6)t.

Another way of looking at this is to notice that in six hours, the air along the middle row of grid points (y=2) will shift one grid point to the east. Similarly, the air along the y=1 grid row will not move since here U=0. Finally, the air along the y=3 grid row will shift two grid points to the right in six hours since here U=2/6 km/hr.

Putting all this together, the grid-point temperatures as a function of t are

$$T(1,1,t) = 2$$
$$T(2,1,t) = 4$$
$$T(3,1,t) = 6$$
$$T(1,2,t) = 0 - (2/6)t$$
$$T(2,2,t) = 2 - (2/6)t$$
$$T(3,2,t) = 4 - (2/6)t$$
$$T(1,3,t) = -2 - (4/6)t$$
$$T(2,3,t) = 0 - (4/6)t$$
$$T(3,3,t) = 2 - (4/6)t$$

where again t is in hours and T is in °C. Fig. 2-3 shows the isotherms and grid-point values for this forecast.

2. Spectral Method

To get this same forecast in spectral form we use the same reasoning we just used in the grid-point method. That is, we add the present temperature to the temperature advection. From equation (1) we already know the

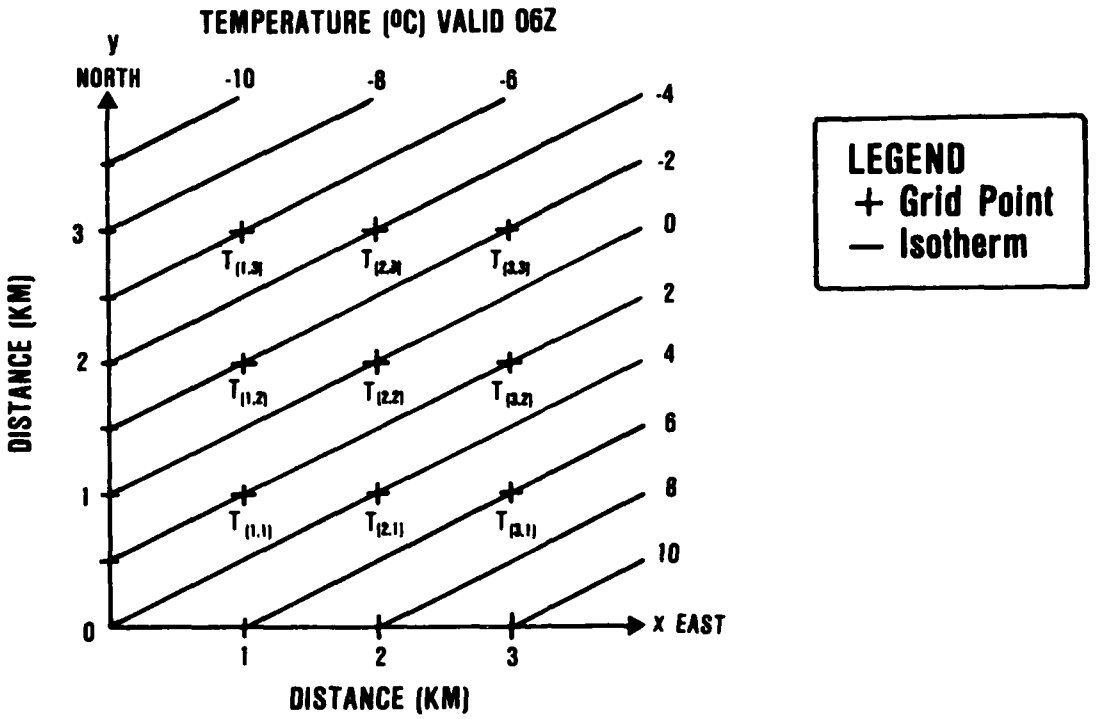

Fig. 2-3. Forecast temperature field valid at 06Z.

current temperature. Furthermore, we know that the temperature advection is the east-west temperature gradient times the u-compontent wind. From Fig. 2-1, the east-west temperature gradient is 2°C/km*, and from equation (2), the u-compontent wind is (y-1)(1/6 km/hr). Thus, in spectral form, the forecast for T is

$$T(x,y,t) = \underbrace{(2+2x-2y)}_{\text{present temperature (°C)}} - \underbrace{2}_{\text{east-west temperature gradient (°C/km)}}\underbrace{(y-1)}_{\text{u-component wind (1/6 km/hr)}}t \qquad (3)$$

Again, the advection term is negative because the wind is bringing in cold air.

---

* Those of you familiar with calculus will recognize this to be d/dx of equation (1).

Just to be sure that we got this equation right, let's see what the temperature at x=2, y=3 should be in six hours:

$$T(2,3,6) = 2^{o}C + (2^{o}C/km)(2\ km) - (2^{o}C/km)(3\ km) - (2^{o}C/km)(3-1)(1/6\ km/hr)(6hr)$$

$$= 2 + 4 - 6 - 4$$

$$= -4.$$

Compare this with the grid-point method:

$$T(2,3,6) = 0 - (4/6)(6)$$

$$= -4.$$

This simple example points out one of the main advantages of using a spectral model. That is, we can define a physical processes such as advection, for the entire field, with just one equation. When we use the grid-point method we must uniquely define the advection term for all nine grid points. This is why spectral methods generally take much less computer time than grid-point methods.

3. A Six-hour forecast

Using the two different methods, let's make a complete six-hour forecast for this temperature field. First, via the grid-point method, the forecast temperatures at 06Z would be

$T(1,1) = 2$
$T(2,1) = 4$
$T(3,1) = 6$
$T(1,2) = -2$
$T(2,2) = 0$
$T(3,2) = 2$
$T(1,3) = -6$
$T(2,3) = -4$
$T(3,3) = -2.$

The same forecast via the spectral method would be

$$T(x,y) = 2x - 4y + 4. \qquad (4)$$

Again, equation (4) is still the equation of a plane.

D. The Next Analysis

Now let's suppose that a new set of temperature observations is taken at 06Z as shown in Fig. 2-4. Although none of these observations falls directly on a grid point, the observations do indicate that the grid-point forecasts are slightly in error. That is, if you interpolate the observed values to the grid points in row two, you will find that the forecast temperatures are

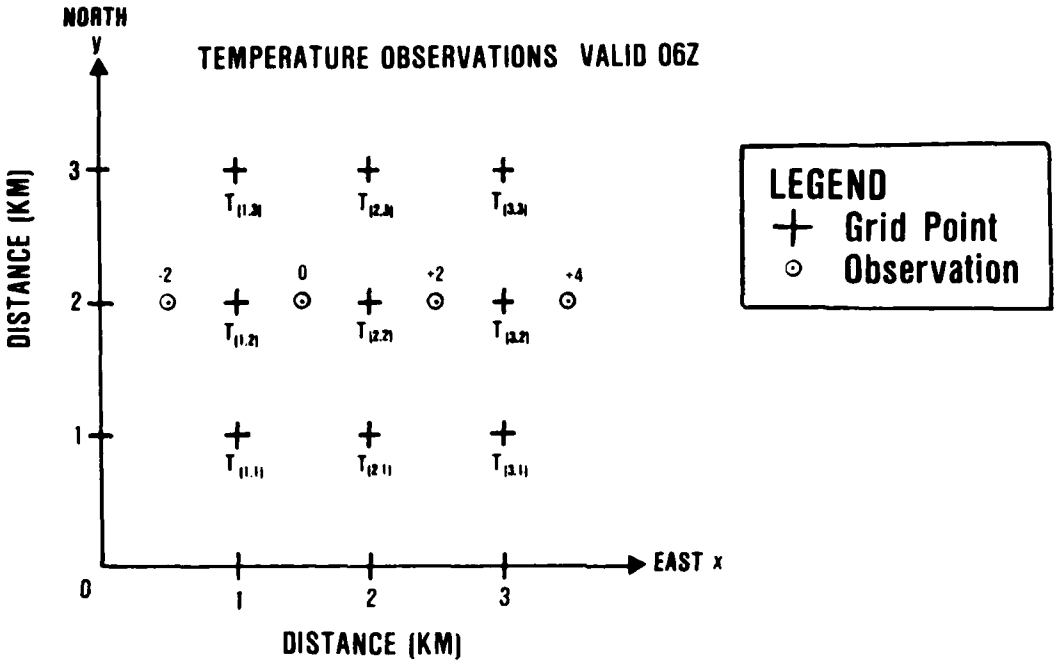

Fig. 2-4. Temperature observations taken at 06Z.

one degree too cold.

We thus find ourselves in a dilemma. Should we add one degree to the forecast for all nine grid points, or should we only adjust the three grid points in the middle row? The AWAPS numerical analysis scheme adjusts only the middle row. The rule is, if a grid point has observations nearby, it is corrected; however, if there are no nearby observations, the forecast remains unchanged. Using this rule, the new analysis grid-point values for 06Z would be

```
T(1,1) = 2
T(2,1) = 4
T(3,1) = 6
T(1,2) = -1
T(2,2) = 1
T(3,2) = 3
T(1,3) = -6
T(2,3) = -4
T(3,3) = -2.
```

Fig. 2-5 shows this graphically.

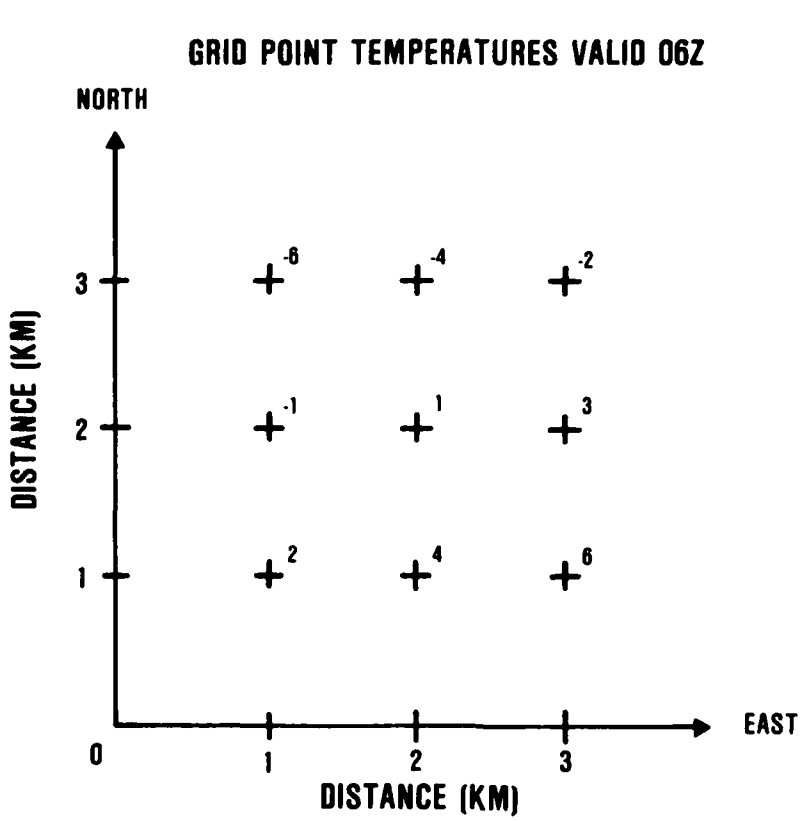

Fig. 2-5. Grid-point temperatures using forecast values for rows 1 and 3 and interpolated observations for row 2.

Under this grid-point analysis scheme, the new observations do not pose much of a problem. However, if we wish to put this new temperature field into spectral form, we will have to make some compromises, especially if we confine our representation to the equation of a plane. The equation of a plane was fine as long as the field itself was in this form. But the grid-point temperatures in Fig. 2-5 no longer fall in the same plane. Therefore, there is no single equation of a plane that can perfectly model these temperatures.

For the sake of illustration, let's assume that our computer model can only accept the equation of a single plane. Therefore, we must do the best we can to represent the field in this form. The simplest way would be to merely shift all the isotherms northward as shown in Fig. 2-6. This would mean that none of the grid-point temperatures would be represented perfectly, but that the overall error would be smaller. The equation representing this "best fit" plane would be

$$T = 2x - 4y + 4.3. \qquad (5)$$

You will notice that the only difference between equations (4) and (5) is in the last term.

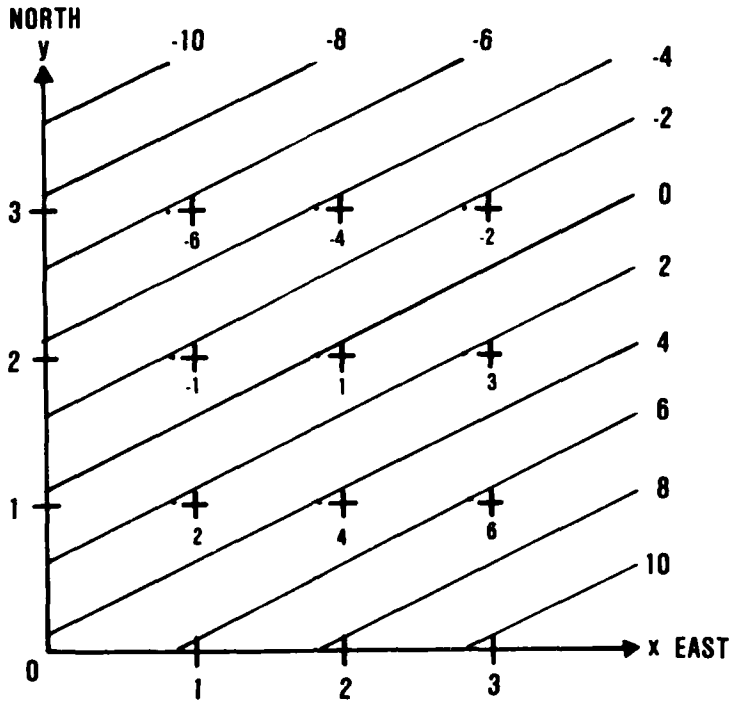

Fig. 2-6. Grid-point temperatures and "best fit" temperature plane.

E. Data Assimilation

Once we've done this 06Z analysis we begin the process all over again. We make a six-hour forecast (first guess) valid at 12Z and then use the 12Z observations to correct this first guess. This corrected first guess becomes the new analysis, and so on.

This process of making a forecast, updating it with new observations, then making a new forecast, etc., is called data assimilation. The HIRAS is such a data assimilation system.

F. Waves and Spectral Coefficients

In the above example we used the equation of a plane to simulate a spectral representation. A true spectral representation actually uses sines and cosines. That is, a spectral equation contains a series of terms, each having either a sine or cosine as a factor.

You will recall that sine and cosine curves look like waves. That's why we often speak of a spectral representation in terms of waves. For example, the operational GSM is a "40-wave" spectral model.

Now, the equation for a given field in the 40-wave GSM contains a lot more than 40 terms. In fact, to represent a single variable at just one level, the 40-wave GSM needs 3,444 terms. This is because we're dealing with waves in two dimensions and each wave in each dimension contains both a sine and a cosine. Furthermore, for mathematical reasons, the 40-wave model has 41 sines and cosines in one dimension and 42 sines and cosines in the other. Thus, the 3,444 terms come from the product: 41 X 42 X 2. The 2 appears in this product because we have both a sine and cosine (2 terms) for each wave.

Each of these 3,444 terms will also have a constant as a factor. These constants are called spectral coefficients and determine the amplitudes of the individual waves. Basically, a spectral representation chooses the coefficients that produce the overall "best fit" of the observed field. In other words, it chooses the coeffients that minimize the overall error in representing that field. The rule of thumb is, the more waves you use, the higher the resolution and the smaller the overall error.

To get a better idea of what a spectral coefficient is, let's go back to equation (5). Here we have three terms, each containing a constant. For this equation, the spectral coefficients are these constants, 2, 4, and 4.3.

For a more detailed description of the GSM spectral coefficients, see Sela (1982).

G. Summary of Key Points

Although the examples in this chapter are much simpler than the actual AWAPS models, they do illustrate several key points about NWP. These include:

1. No numerical analysis is exact. It is, rather, a combination of a first guess and some type of interpolation scheme that uses observations to correct that first guess.

2. In a grid-point analysis, a given observation affects only the nearby grid points.

3. A spectral analysis tries to fit a specific equation to <u>all</u> the observations. That is, each observation affects the entire analysis.

4. In the absence of any observations, the forecast becomes the analysis.

5. A given field can be represented quite accurately by either the grid-point or spectral method. In fact, a set of grid-point values can be converted to spectral notation and vice versa.

Chapter 3 - AWAPS Production Cycle

A. General

In Chapter 2 we saw the difference between an analysis and a forecast model. In this chapter we will see how the AWAPS analysis and forecast models are linked together into a production cycle.

B. Global Production Cycle

Fig. 3-1 shows how the HIRAS and GSM are linked together to produce a global 0-96 hour forecast every six hours. The upper portion of this diagram represents the HIRAS, while the lower portion represents the GSM.

As we saw in Chapter 2, the HIRAS is a data assimilation system that includes both a first guess and an analysis model. The first-guess model in HIRAS is merely a 30-wave version of the GSM.

The HIRAS portion of Fig. 3-1 shows how the first-guess model and the analysis constantly feed each other. Each six hours the first guess is corrected using current observations. This new analysis starts the process all over again, as it provides the initial conditions for the next six-hour first guess.

The GSM portion of Fig. 3-1 shows the heart of the AWAPS, the operational global forecast model. This particular model is a 40-wave, 12-layer GSM.* It also uses the HIRAS analysis for its initial conditions. Instead of producing just a six hour forecast, however, it produces the full 0-96 hour forecast. All the operational global forecasts that come out of the AWAPS come from this GSM.

C. RWM Production Cycle

The RWM has not yet been integrated into the AWAPS production cycle. As we will see in Chapter 6, the RWM is designed so it can forecast anywhere at anytime. Therefore, the specific areas and times for the RWM will be dictated by operational requirements.

In spite of this great flexibility, the RWM will most likely also be run routinely over three fixed windows at specified times during the day. These windows will be over North America, Europe, and Asia. The specific times and coverages are yet to be determined.

---

* We will discuss model layers in Chapter 5.

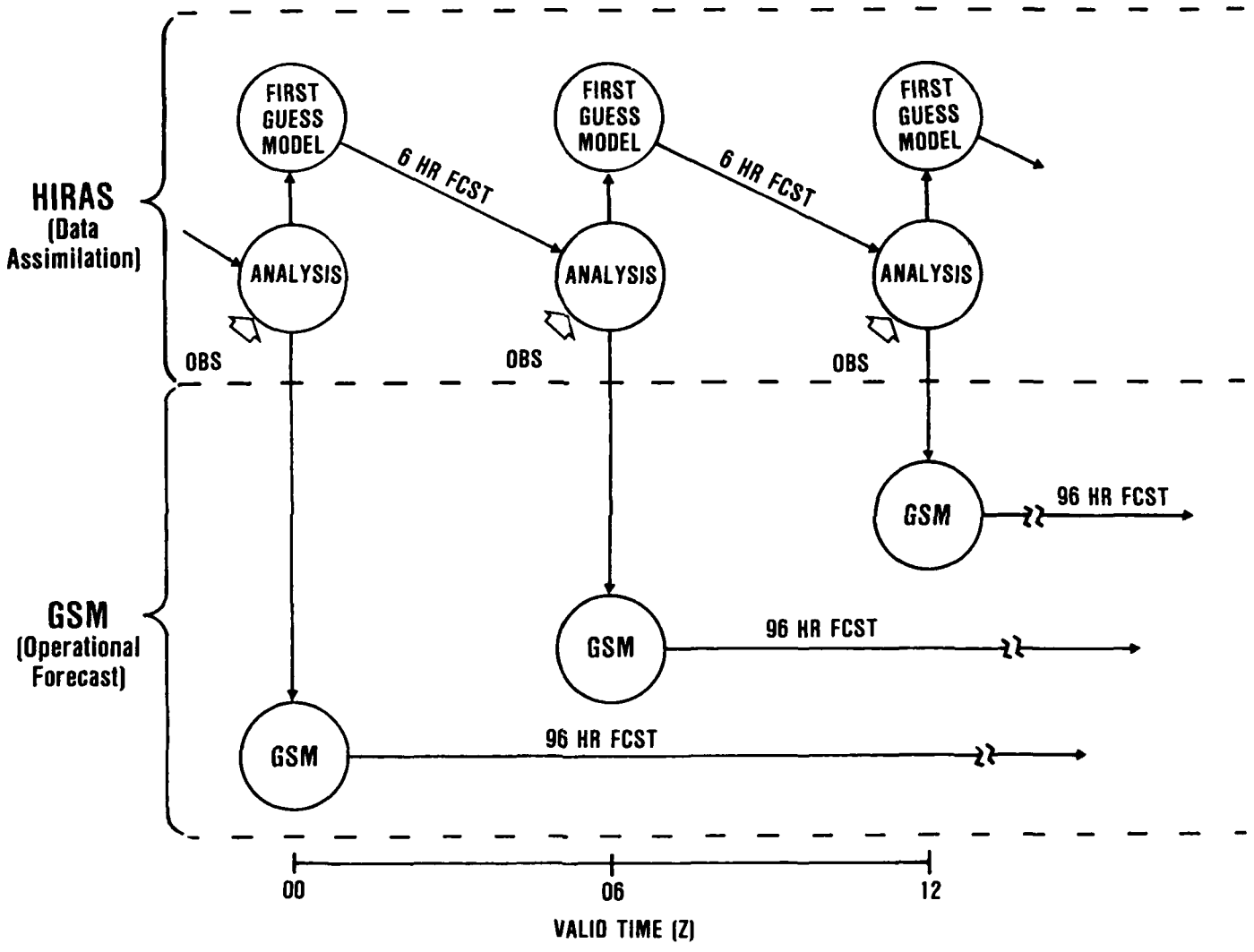

Fig. 3-1. HIRAS-GSM production cycle.

The way the RWM interfaces with the other AWAPS models is also still under consideration. One method would have the RWM feed directly off the HIRAS analysis just like the GSM. Another method would have the RWM receive the HIRAS first guess and then do its own analysis using the same grid it will use in its forecast.

Chapter 4 - HIRAS

A. General

The HIRAS is the primary analysis system in AWAPS. It produces global analyses on a 2.5 X 2.5 degree latitude-longitude grid (Fig. 4-1). To do this it uses a variety of observations taken from land stations, ships, buoys, aircraft, balloons (RAOBs), and satellites.

As we saw in Chapter 3, the HIRAS has two main components, a first-guess model and an analysis model. Since the first-guess model is just another version of the GSM, we will wait until Chapter 5 to discuss it. Here we will concentrate on the analysis portion of HIRAS.

B. Optimum Interpolation

The HIRAS uses an analysis technique called optimum interpolation (OI). The model itself is an adaptation of the OI analysis used at NMC. Dey and Morone (1985) give a detailed description of the NMC system. Stobie, et al., (1985) describe how the AFGWC OI differs from the NMC version.

Basically, OI takes into account three factors: (1) the distance between the observations and the grid point, (2) the accuracy of the observing instruments, and (3) the expected accuracy of the first guess. Appendix A contains a detailed description of the mechanics of OI. Without getting into these details, here is conceptually how the HIRAS uses these three factors.

1. Distance Between the Observation and the Grid point

This is the foundation of nearly every numerical analysis scheme. It [illegible]. Basically, what the model does is to assign weights to [illegible] during each grid point. Each observation is allowed to affect the analysis according to how close it is to the grid point [illegible] observations generally will differ.

[illegible] an example of how two observations might affect the [illegible] grid point. In this figure the first-guess temperature at the grid point is +1°C. The analysis and the first-guess at the observation B differ by 2°C, while the analysis differs by 3°C. Below the figure is a graph of a typical weight vs. distance function. Using this graph, observation A should receive a weight of 0.5 and observation B a weight of 0.25. The new correction applied to the analysis would thus be

$$\text{correction} = (0.5)(+2^{\circ}C) + (0.25)(-2^{\circ}C)$$

$$= +0.5^{\circ}C.$$

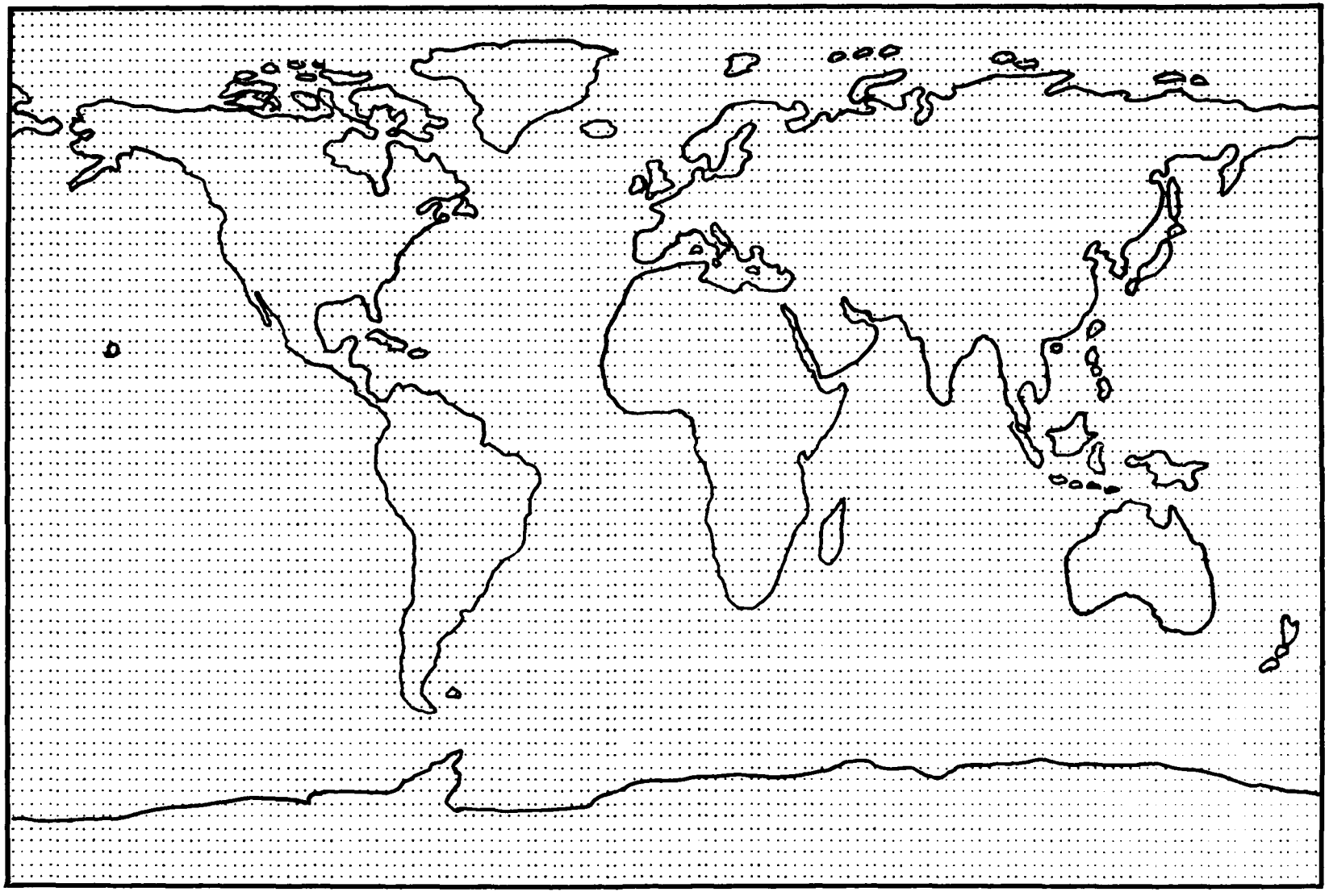

Fig. 4-1. 2.5 X 2.5 degree latitude-longitude grid.

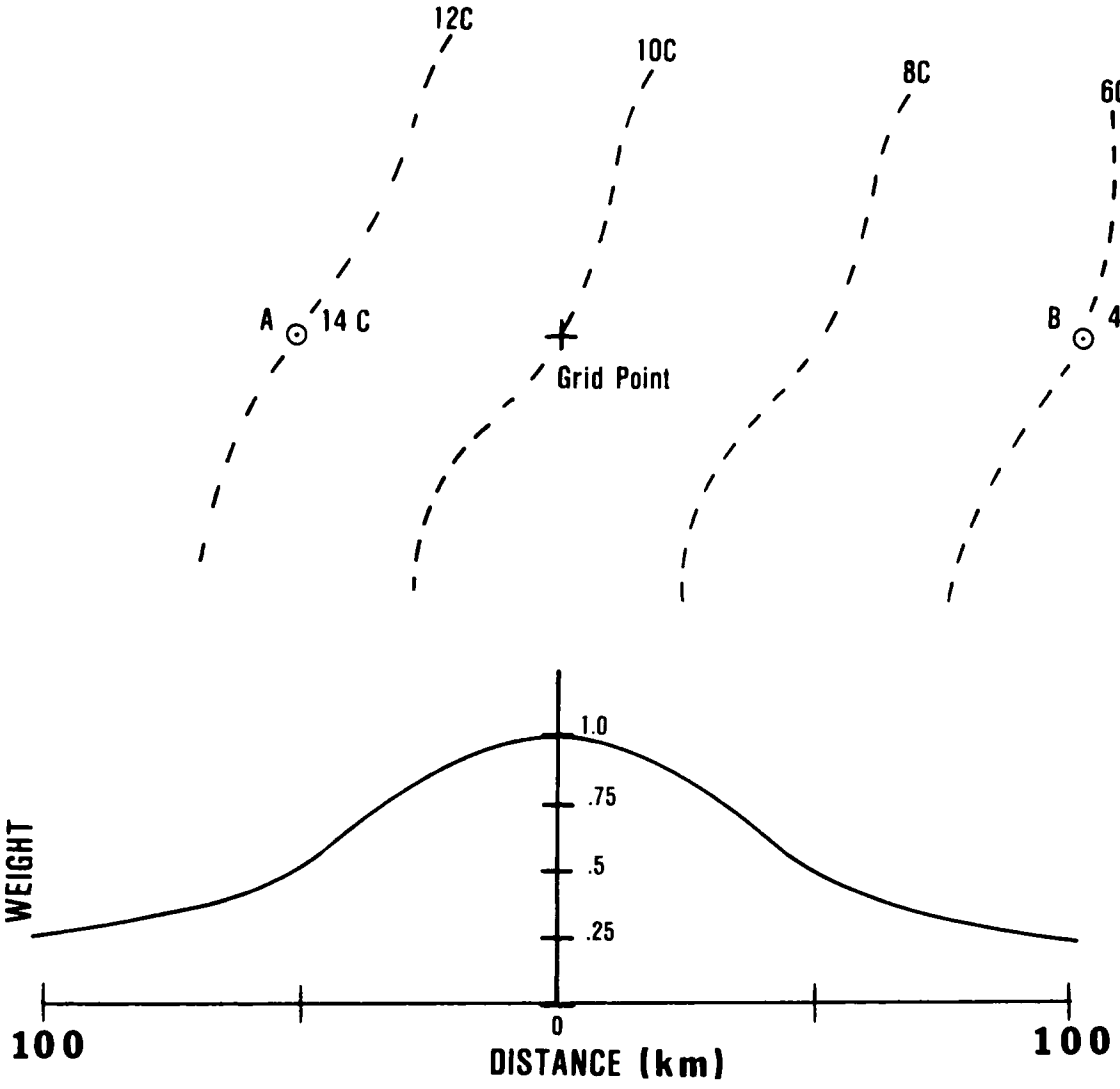

Fig. 4-2. Temperature analysis using a first guess (dashed lines) and observations (A & B). Below the grid point is a "weight vs distance" function used to determine how much weight each observation should receive in correcting the first guess.

Therefore, the final analysis at the grid point would be

final analysis = first guess + correction

= 10°C + 0.5°C

= 10.5°C.

This example is a bit over-simplified. The OI actually uses more than this horizontal "weight vs distance" curve to determine its weights. It also looks up and down for observations, incorporating a separate vertical weighting scheme. The basic principle, however, is still the same: the closer the observation is to the grid point, the more weight it receives.

2. Accuracy of the Observing Instruments

One of the major advantages of OI is its ability to distinguish between various instruments. This is especially critical in this day of satellite soundings, cloud-track winds, aircraft wind reports, etc.

The way OI takes the instrument errors into account is to assign every instrument type a unique expected error. These errors are determined statistically. The basic OI rule is: the lower the expected instrument error, the more weight that observation will receive. For example, a 500 mb temperature from a RAOB is probably more accurate than a 500 mb temperature from a satellite. Thus, if these two observations are the same distance from the grid point, HIRAS will automatically give the RAOB more weight.

Fig. 4-3 shows the instrument errors currently used in HIRAS. These error values came from the European Center for Medium Range Weather Forecasts. Again, the larger the instrument error, the less weight that observation is allowed to receive.

3. Accuracy of the First Guess

Each HIRAS analysis produces two types of fields, analyses and errors. The analyses are the standard grid-point analyses we described in Chapter 2. The error fields, however, are specialized fields unique to OI. These error fields indicate how accurate the analysis is at each grid point. Basically, the more observations you have, the better your analysis, and thus, the lower the expected error. Fig. 4-4 is a sample HIRAS error field. Notice that over data-rich areas such as North America and Europe, the error values are low, while over data-sparse areas such as the Indian Ocean, the error values are large.

Besides indicating how accurate the analysis is, the analysis error fields also dictate the accuracy of the first guess. To see how this works, let's consider two areas, North America and the South Pacific.

Over North America there are many RAOB stations that take observations every 12 hours. Because of this, the analysis over North America is quite accurate. The first guess over North America is, in turn, also quite accurate.

Over the South Pacific, on the other hand, there are very few RAOBs. Occasionally there will be a satellite pass which will provide some data, but never as good as the RAOB network over North America. Therefore, the initial conditions over the South Pacific are usually poor. Thus, the first guess over the South Pacific is probably not as accurate as the first guess over North America.

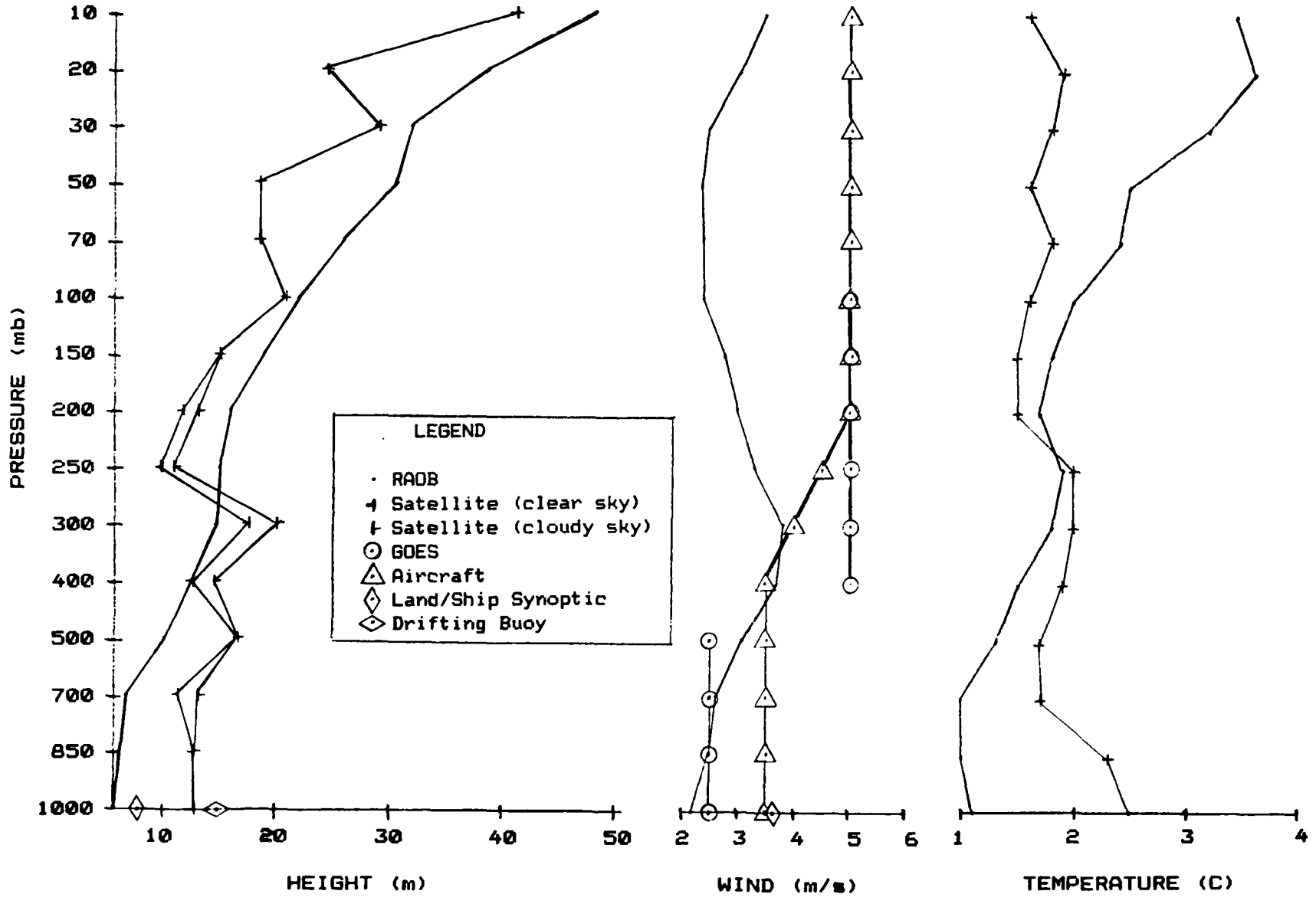

Fig. 4-3. HIRAS instrument errors.

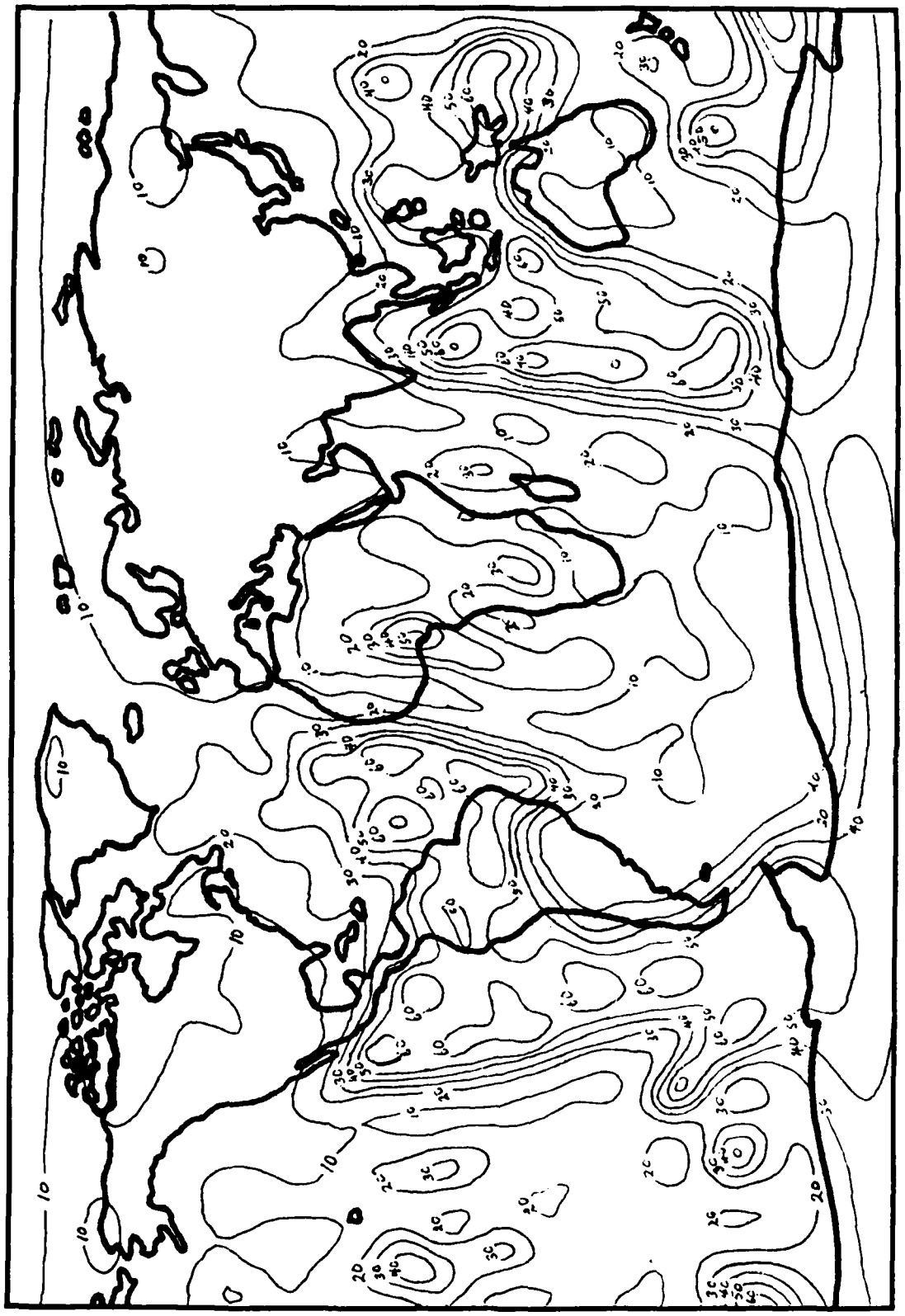

Fig. 4-4. Sample HIRAS 250 mb height error field (m).

Because of this difference in the accuracy of the first guess, HIRAS believes the first guess over North America more than it does over the South Pacific. How does it do this? It simply varies the degree to which it "draws" for the observations. Specifically, it does not allow an observation to affect the analysis as much over North America as it does over the South Pacific. For example, with all other factors being equal, suppose we have a RAOB over North America whose temperature differs from the first guess by 5°C. Since the first guess over North America is considered quite accurate, the HIRAS may choose to only adjust the first guess by 3°C. In the South Pacific, however, where the first guess is probably much worse, the same 5°C difference may result in a 4°C adjustment.

This scheme often causes a great deal of consternation when it is first explained to a forecaster. The usual question is, "Why do we correct less for the observations over North America where the data are good, and more for the observations over the South Pacific where the data are much worse?" The answer is, the OI is a combination of both the observations and the first guess. The better the first guess, the less weight you should give the observations. Keep in mind that the observations are not perfect either. That RAOB that tells you to correct 5°C may actually have a 2°C error of its own. If the first guess in the vicinity of that RAOB has an expected error of only 1°C, it would not make much sense to give the observation more weight than the first guess.

Finally, the analysis and first-guess error fields are constantly evolving. Over data-rich areas such as North America, Europe, and Asia, the analysis errors stay relatively low. Over the data-sparse areas such as the oceans and most of the Southern Hemisphere, the analysis errors remain relatively large.

C. Analysis Fields

The HIRAS ultimately produces 14 different fields, but it directly analyzes only five: heights, u-component winds, v-component winds, temperature, and specific humidity. All the other HIRAS fields are derived from these five basic fields. Appendix B contains a list of the HIRAS fields along with the methods used to derive them.

The HIRAS height analysis uses a scheme known as multivariate OI. That is, it uses both height and wind observations to correct the first guess. It does this by assuming the height and wind observations are in geostrophic balance.*

The wind analysis is also multivariate. In fact, for a given grid point it uses the same set of observations used by the height analysis.

The only exception to this multivariate height-wind analysis is in the tropics. This is because near the equator the geostrophic assumption is no

---

* Geostrophic balance occurs when the pressure gradient force is in balance with the Coriolis force.

longer valid. Therefore, equatorward of 15 degrees latitude, the height and wind analyses are done independently. That is, only height observations affect the height analysis and only wind observations affect the wind analysis. This is commonly referred to as a univariate analysis.

The temperature and specific humidity analyses are univariate everywhere. That is, the temperature analysis uses only temperature observations and the specific humidity analysis uses only moisture observations.*

D. Upper-Air vs Surface Analysis

The HIRAS analysis is composed of two distinct modules, a surface module and an upper-air module. The upper-air HIRAS is the real workhorse of the system, as it provides all the initial conditions for the GSM. The surface HIRAS serves only one function, to anchor the satellite soundings for the upper-air analysis.**

1. Upper-Air Analysis

We've already said that the HIRAS does an OI grid-point analysis on a 2.5 X 2.5 degree latitude-longitude grid (let's call it the "2.5 grid"). Inside the upper-air model, however, there is a bit more to it than that. For one thing, the internal grid is not as high a resolution as the 2.5 grid. Secondly, the upper-air analysis uses a spectral transformation in addition to the OI. To understand this, let's look at the step-by-step upper-air analysis process.

The first step in the process is to convert the first-guess fields into grid-point values. These fields come out of the first-guess model as 30-wave spectral coefficients. The HIRAS converts these coefficients to its own analysis grid shown in Fig. 4-5.

Notice that the grid in Fig. 4-5 is not the 2.5 grid. It has a coarser resolution with only 1/3 as many grid points as the 2.5 grid. The HIRAS does its grid-point analysis on this coarser grid to save computer time.***

---

* Moisture observations include dewpoint, dewpoint depression, relative humidity, and specific humidity. The HIRAS moisture analysis converts all of these to specific humidity before it performs its specific humidity analysis.

** Satellite soundings consist of a series of thickness values. In order to convert these thicknesses to heights, you must first determine the base height of the sounding. This base height is derived from the surface analysis and is referred to as the "anchor" or "reference level."

*** Numerical modelers refer to this as an "equal-area Gaussian grid," or "Kurihara grid." Its main advantages over the 2.5 grid are (1) its resolution is nearly constant from pole to equator and (2) its latitudes (Gaussian latitudes) make it easier to convert from grid-point to spectral representation. (Kurihara and Holloway, 1967)

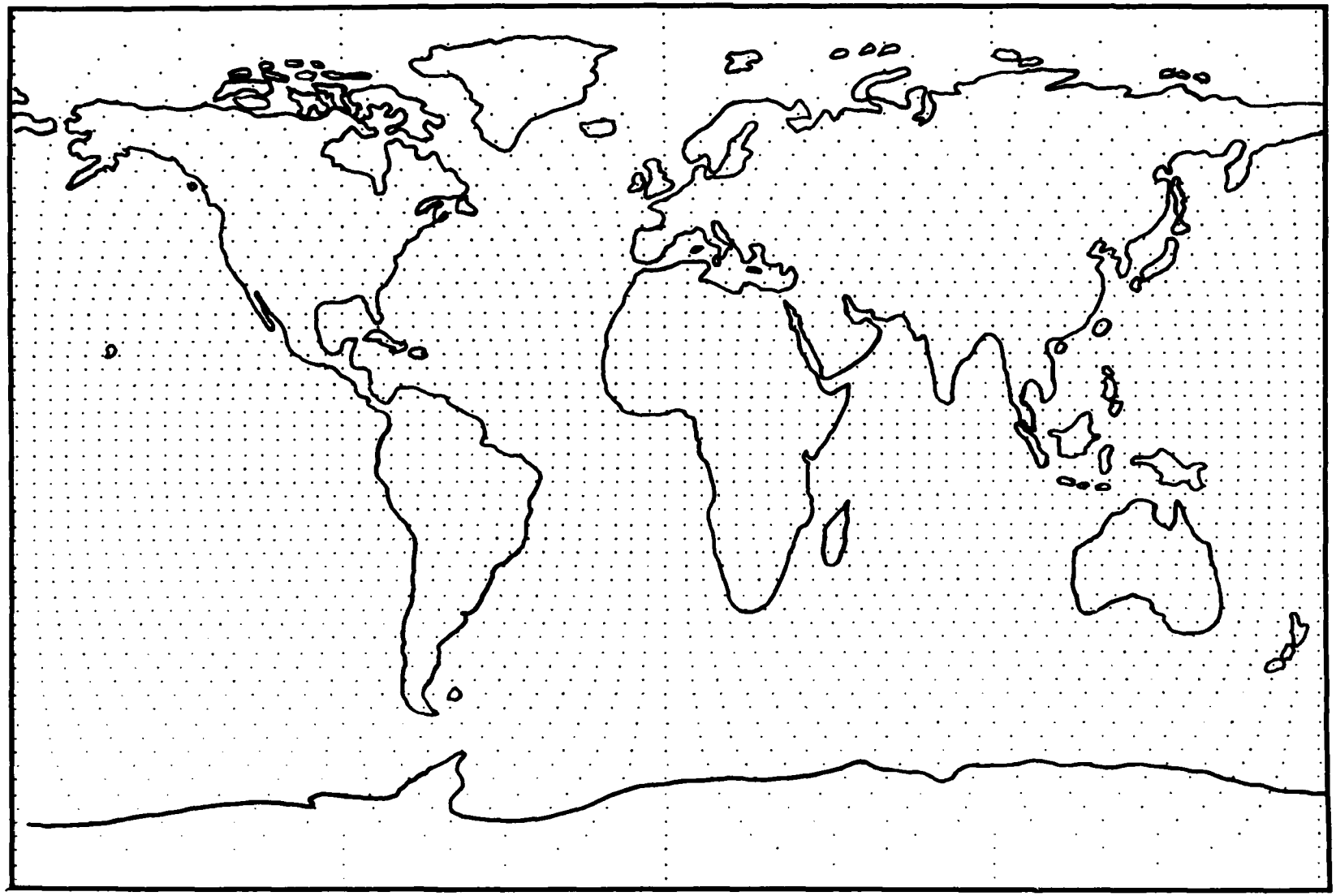

Fig. 4-5. Internal HIRAS upper-air analysis grid.

Once the first guess is converted to this grid, the analysis model performs its OI. Next, this grid point-analysis is transformed back to 30-wave spectral coefficients. This last step is important. It means that although the upper-air HIRAS is basically a grid-point analysis, it still includes a spectral transformation. The AFGWC forecasters should be particularly aware of this, because it means that every observation (including bogus) affects every grid point in the world.

The final step in the upper-air analysis is to convert these 30-wave spectral coefficients to the 2.5 grid. Again, even though the analysis appears on this grid in the AFGWC data base, the true resolution of the analysis is the grid shown in Fig. 4-5.

a. Stratospheric Analysis

Because of some of the shortcomings of the first-guess model in the stratosphere (above 100 mb), the HIRAS must make some special compensations. First, it does not use the first-guess forecast model above 100 mb. Instead, it uses the previous analysis for its first guess. Second, it forces the first-guess winds to be geostrophic above 100 mb. Finally, it uses only a horizontal OI in the stratosphere. For example, the 30 mb analysis uses only 30 mb observations.

Fig. 4-6 shows the various HIRAS analysis levels and how much they can look up or down for observations. Notice the "barrier" near 100 mb. This barrier is imposed mainly because the stratospheric first-guess corrections (observation - first guess) are not necessarily correlated with the tropospheric corrections (Carr and Tuell, 1985).

2. Surface Analysis

Like the upper-air HIRAS, the surface HIRAS is an OI model. It has three main characteristics that distinguish it from the upper-air HIRAS: (1) its analysis grid, (2) the way it uses the error fields, and (3) the way it uses observations to correct the first guess. As for the grid, the surface HIRAS performs its analysis directly on the 2.5 grid. It does not use any spectral transformation or special internal grids. Furthermore, the surface analysis does not use the OI error fields at all. Instead, it "believes" the first guess just as much over the data-rich areas as it does over the data-sparse areas. Because of this, the surface analysis tends to believe the observations a bit more than the upper-air analysis does. Finally, the surface wind and pressure analyses are done univariately. This is done because the geostrophic assumption is just not appropriate near the earth's surface.

E. The Analysis Cycle

In Fig. 3-1 we saw the overall HIRAS-GSM production cycle. Now let's focus on the analysis cycle.

As you can see in Fig. 4-7, every six hours the HIRAS does three surface analyses and two upper-air analyses. The earlier analyses are done to meet

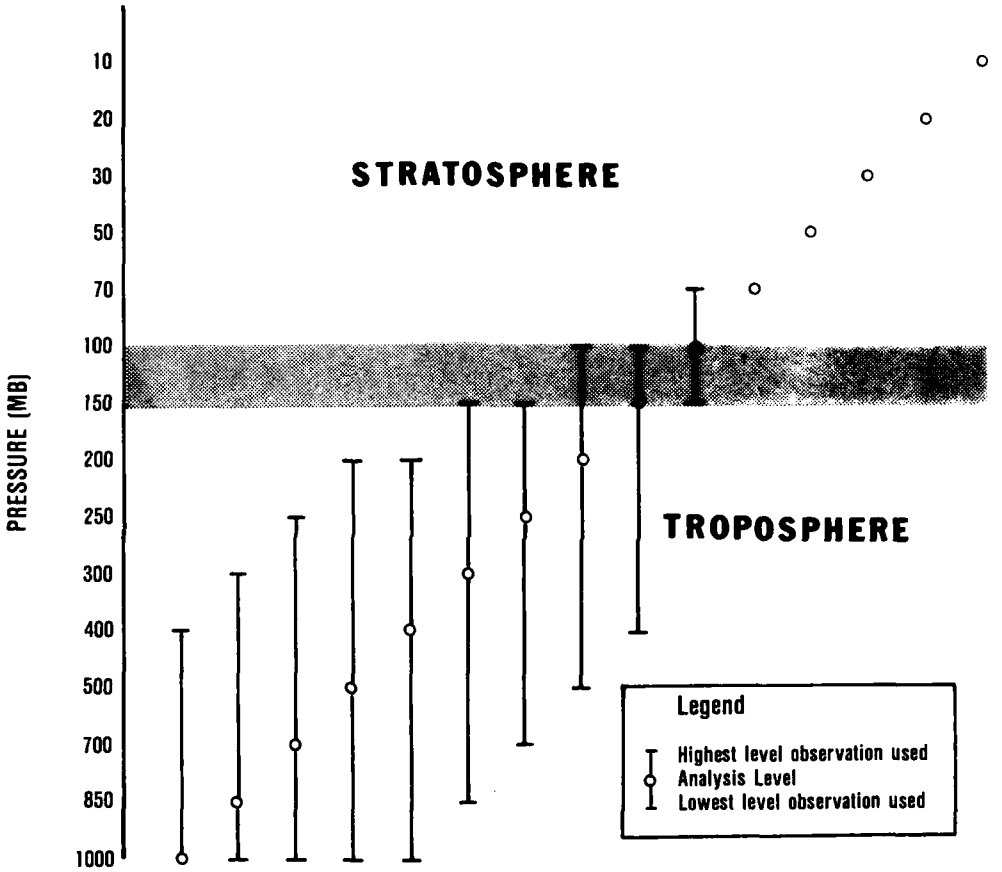

Fig. 4-6. HIRAS vertical interpolation limits.

customer requirements, while the later analyses are done to take advantage of late-arriving data. This cycle also gives the AFGWC forecasters a chance to quality control (QC) each analysis. To see how this all fits together, let's step through the 00Z cycle.

First, at about 01Z the first-guess model upper-air output is sent to the AFGWC forecasters for QC (#1 in Fig. 4-7). The forecasters have two hours to review this output. If there is anything they don't like, they can generate artificial, or "bogus," data for use in the subsequent analysis. For

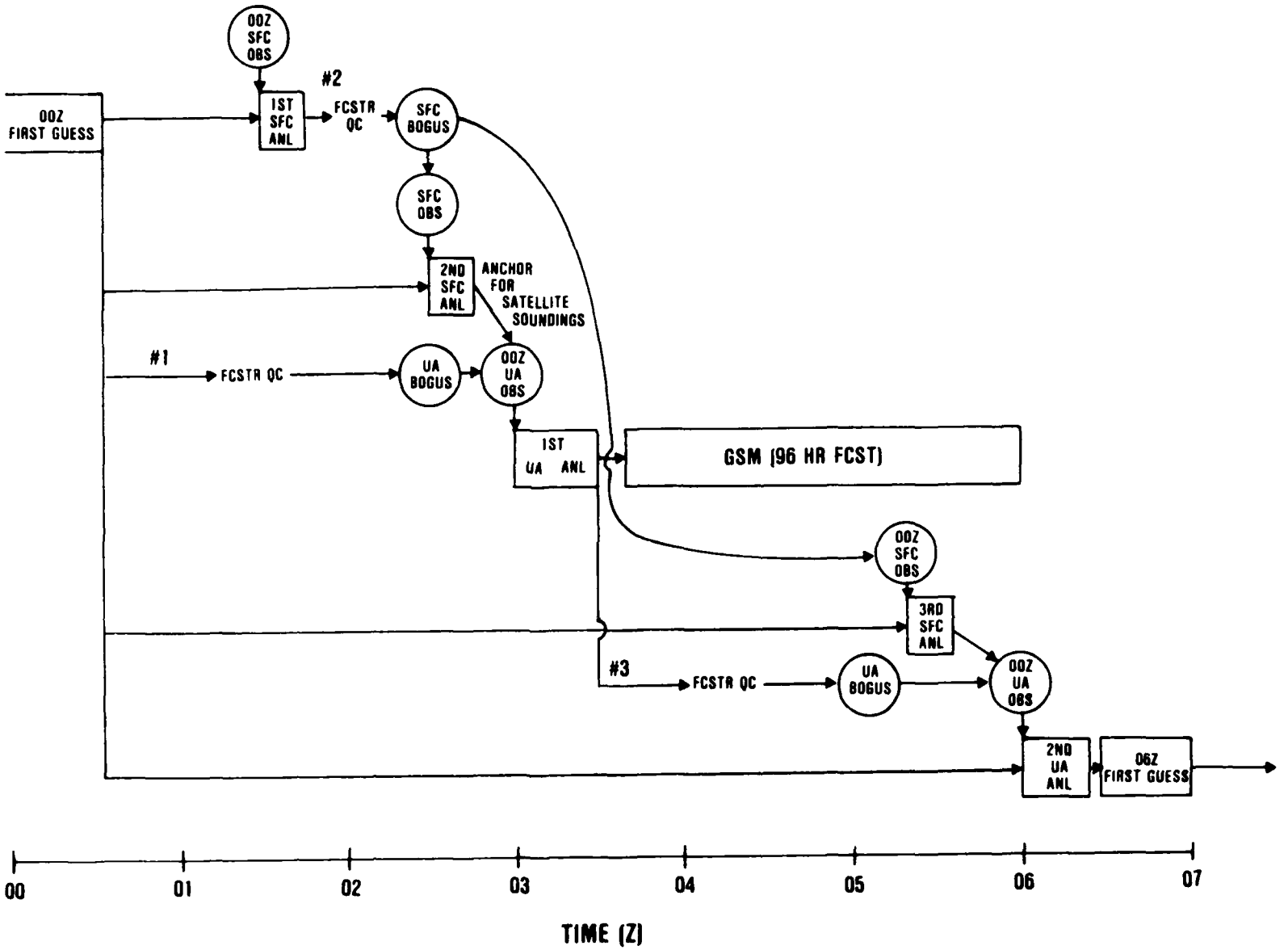

Fig. 4-7. HIRAS analysis cycle. Circles represent data inputs while rectangles represent AWAPS models. The width of the rectangles indicate how long the models take to run on the AWAPS computers.

example, if they believe the first guess has moved an upper-air trough too far east, they might introduce bogus data to move the trough back to the west. The analysis will then use this bogus data to correct the first guess.

At 0130Z HIRAS does its first 00Z surface analysis. This output also goes to the AFGWC forecasters for QC (#2 in Fig. 4-6). In this case they have until 0230Z to prepare bogus observations or to delete real observations that they believe are incorrect.

At 0230Z HIRAS does its second 00Z surface analysis. This analysis anchors the satellite soundings for the first upper-air analysis.

At 0300Z HIRAS does its first upper-air analysis. This analysis uses all the real and bogus data available at that time. This first upper-air analysis provides the initial conditions for the GSM.

During the next three hours, 00Z observations continue to trickle in at AFGWC. To take advantage of this late-arriving data the HIRAS does a second 00Z upper-air analysis at 0600Z. This second upper-air analysis is preceded by a third surface analysis at 0530Z, which re-anchors the satellite soundings. Also, between the first and second upper-air analyses, the AFGWC forecasters may submit more bogus data.

Finally, at about 0630Z, the first-guess model runs using the second 00Z upper-air analysis for its initial conditions. At this point the six-hour cycle begins all over again.

There is one important aspect of this six-hour cycle that AFGWC forecasters should be aware of. That is, the first-guess model always provides the first guess for the analysis. This was not always the case at AFGWC. In fact, when HIRAS was first put on line the second 00Z analysis used the first 00Z analysis as its first guess. This, however, contradicts the statistical premise upon which OI is built.* What this means is that if an AFGWC forecaster enters a set of bogus data for the first analysis, the forecaster should resubmit that same bogus for the second analysis.

F. Automated Quality Control

In addition to the forecaster QC described in the previous section, the HIRAS has its own automated QC system. The main objective of this automated system is to throw out bad observations.

As every forecaster knows, observation errors do occur. Usually a forecaster can spot these errors quite easily. For instance, when you're doing a local-area work-chart and an observation of 990 mb shows up in the

---

* OI uses forecast model performance statistics to determine how much weight to give each observation. If an analysis is used for the first guess, these statistics are meaningless. Furthermore, by using the previous analysis for a first guess, you end up giving the observations more weight than they deserve.

middle of a 1046 mb high, you will probably conclude that the 990 mb observation is wrong. The problem for the HIRAS, then, is to try to reason like a forecaster and toss out such erroneous observations. The HIRAS does this through a two step process.

The first step in this process is called the "gross checks." Here, the HIRAS compares each observation with the first guess. If an observation grossly disagrees with the first guess, it is immediately tossed out. If an observation just barely passes the gross checks, it is flagged for the second check called the "buddy check."

In the buddy check, all the observations that just barely passed the gross checks are compared with their nearby, or "buddy," observations. If one of these flagged observations significantly disagrees with its buddies it is thrown out.

G. Summary of Key Points

Here are some of the key points to remember from this chapter:

1. The actual upper-air analysis grid is a lower resolution than the 2.5 degree latitude-longitude grid (see Figs. 4-1 and 4-5).

2. The upper-air analysis includes a 30-wave spectral transform.

3. The HIRAS analysis uses a 3-dimensional OI. For example, a grid point at 500 mb may use observations anywhere between 200 mb and 1000 mb. The only exception to this is above 100 mb, where the OI only looks horizontally for observations.

4. The HIRAS draws more for individual observations in data-sparse areas than it does in data-rich areas.

5. HIRAS compensates for instrument accuracy.

6. Upper-air wind and height analyses are multivariate everywhere except in the tropics.

7. Upper-air temperature and moisture analyses and all surface analyses are univariate.

8. The first guess in the stratosphere (above 100 mb) is the previous analysis.

9. The first-guess winds in the stratosphere are forced to be geostrophic.

10. The surface analysis is only used to anchor the satellite soundings.

11. The upper-air analysis provides all the initial conditions for the GSM and the first-guess model.

a. The first upper-air analysis is done three hours after data time and feeds the GSM.

b. The second upper-air analysis is done six hours after data time and feeds the first-guess model.

12. The HIRAS data QC includes both automated and manual checks. The manual checks are done by the forecasters at AFGWC by adding bogus observations or deleting real observations.

Chapter 5 - GSM

A. General

The GSM is the heart of the AWAPS. Every six hours it produces forecasts out to 96 hours. It also provides the first guess for the HIRAS. Although the GSM's main purpose is to provide height, wind, and temperature forecast for aviation customers, it also provides a wide variety of other fields. Appendix C contains a complete list of these fields and their associated forecast times.

The AWAPS GSM is essentially the same GSM that NMC has been using since 1980. AFGWC received the GSM from NMC in 1984. For a detailed description of the NMC GSM, including equations, see Sela (1982).

Without getting involved in the GSM's complicated equations, let's try to get a general idea of how the model works. To do this, this chapter is divided into four parts. Section B discusses the model's resolution and its impact on the forecasts. Section C lists the atmospheric processes modeled in the GSM. Section D looks at the model's initialization scheme and its effect on the forecasts. Finally, Section E contains model performance statistics and rules of thumb.

B. Resolution

There are two aspects to the resolution of any model, horizontal and vertical. The horizontal resolution for a grid-point model is the grid spacing. The horizontal resolution for a spectral model is based on the number of waves. The vertical resolution for either type of model is based on the number of model layers.

1. Horizontal Resolution

Since the GSM is a spectral model, its horizontal resolution is expressed in terms of waves. The problem is, most of us are used to resolutions expressed in terms of grid-point distances. In the old AWSPE model, for example, the grid-point spacing was 381 km at 60°N. The question is, "How does the horizontal resolution of a 30-wave GSM compare with this 381 km resolution in the AWSPE?"

In the east-west direction the answer is fairly straight forward. Basically, a 30-wave model can contain up to 30 waves (trough-ridge combinations) on a given latitude circle. In the north-south direction, however, there is much more to it than that. Unfortunately, it is beyond the scope of this report to fully explain the north-south resolution of the GSM.

Perhaps the best way to estimate the horizontal resolution of the GSM is through its own internal grid (Fig. 5-1). This particular grid is matched to a 30-wave spectral resolution and is actually used for some of the internal GSM calculations. Its north-south resolution is approximately 270 km and its east-west resolution (at 35°N) approximately 350 km.

As we mentioned in Chapter 3, the AWAPS uses two versions of the GSM, a 30-wave for the HIRAS first guess and a 40-wave for the operational forecasts. But, both of these models store only 30 waves of data in the AFGWC data base. Therefore, for display purposes, the resolution of the 30-wave and 40-wave GSMs is essentially that shown in Fig. 5-1.

The obvious question is, "If you don't save the full 40-waves, why bother with a 40-wave model at all?" The simple answer is, the 40-wave forecast model is more accurate than the 30-wave model. But a 40-wave display is virtually identical to a 30-wave display (Warburton, 1982). In other words, throughout the time integration in the model, the higher number of waves does make a difference, but for a given display, only the first 30 waves are really needed.

Finally, the important point to remember about horizontal resolution is how it limits the forecast. Basically, it determines the smallest scale feature that the model can possibly forecast. Thus, as shown in Fig. 5-1, the smallest scale feature you can expect the GSM to resolve at 35°N would be 270 km long (north-south) and 350 km wide (east-west).*

2. Vertical Resolution

Both the operational GSM and the first-guess model have 12 vertical layers. These 12 layers are positioned via a scheme known as "sigma coordinates." Sigma coordinates vary according to the terrain and, unlike isobaric coordinates, never intersect the ground. They are specified using the equation:

$$\text{sigma} = 1 - P/P_{sfc}$$

where P is the pressure level and P_{sfc} is surface pressure (Phillips, 1959). Fig. 5-2 shows the position of the GSM's 12 sigma layers as they would appear in a standard atmosphere over the ocean.

Notice in Fig. 5-2 that the sigma layers are closer together near the jet stream (~250 mb). This is because the GSM is primarily an aviation forecast model and ~250 mb is where most aircraft fly.

Also notice in Fig. 5-2 that there are only two layers in the stratosphere (above 100 mb). This is one of the reasons why the GSM is not

---

* This is true for a feature such as a surface low or an upper-level trough. But if the feature is a complete wave (trough-ridge combination) then the smallest scale is double these numbers or 540 km north-south and 700 km east-west.

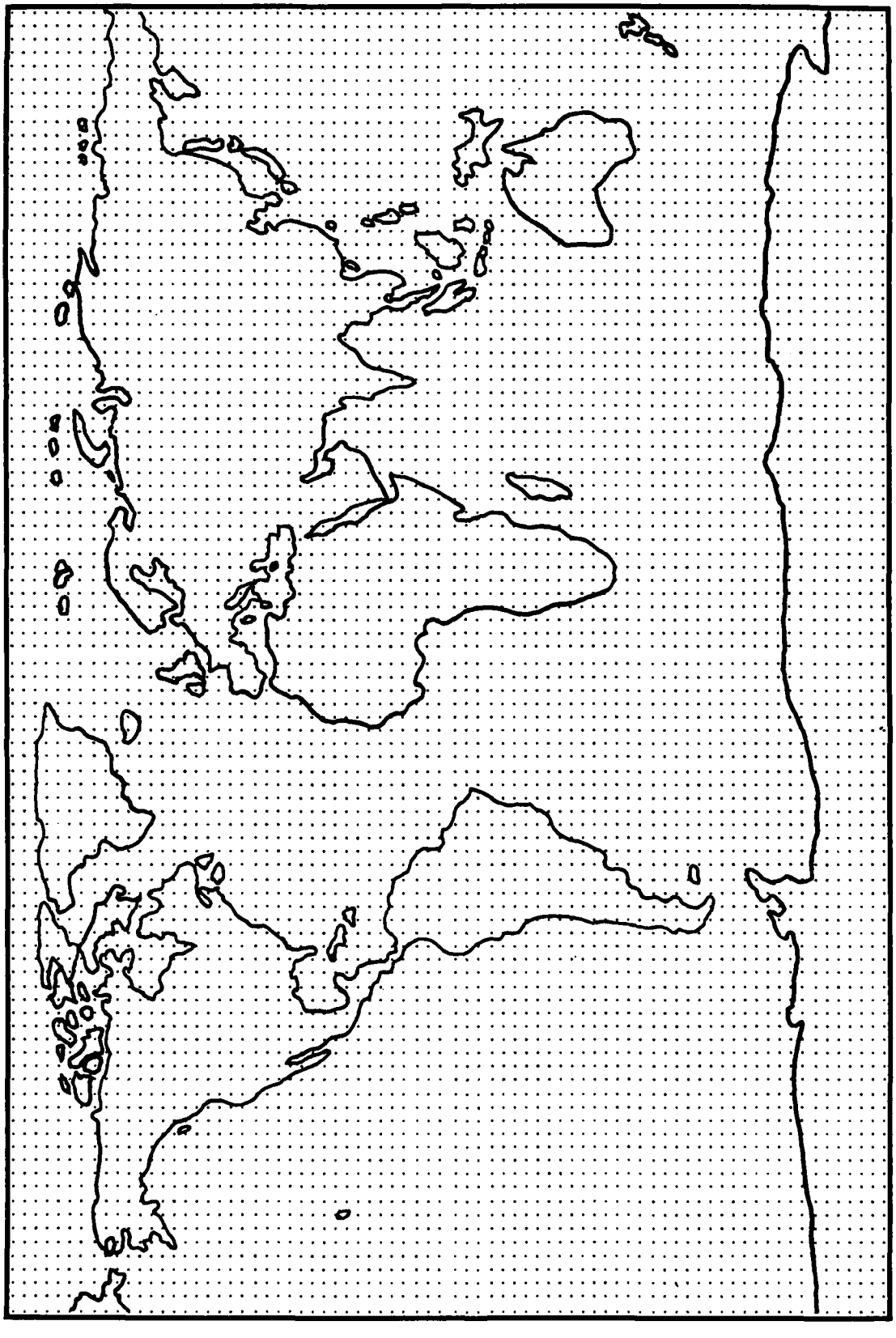

Fig. 5-1. 30-wave GSM grid.

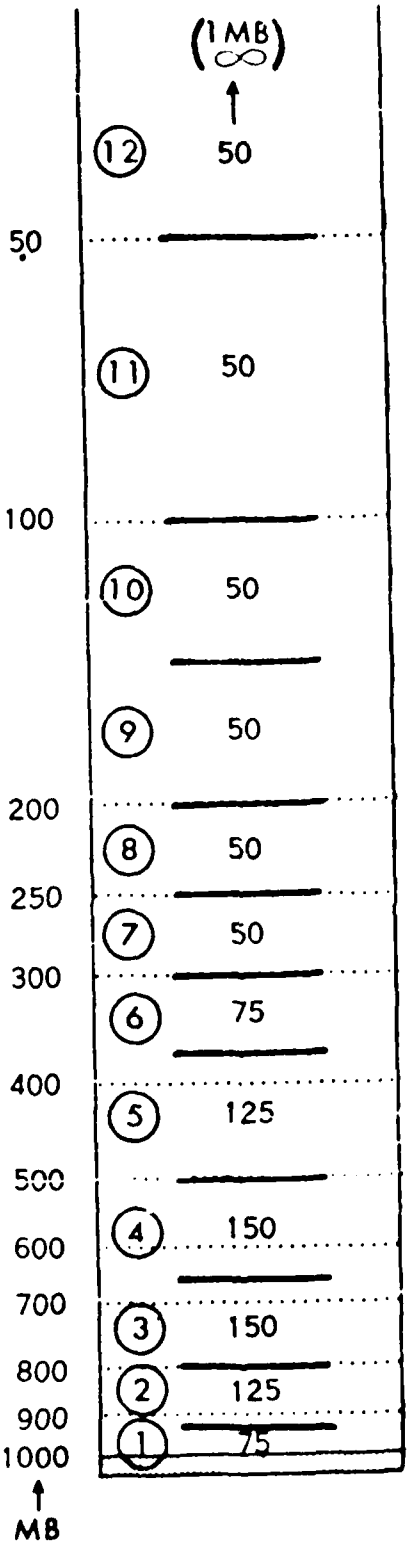

Fig. 5-2. GSM sigma layers (Sela, 1982).

considered a stratospheric forecast model. In fact, AFGWC does not currently have a stratospheric forecast model. Instead, all AFGWC stratospheric forecasts are merely copies of the latest HIRAS analysis.

C. Atmospheric Processes Modeled by the GSM

Like the older PE models, the GSM is also based on the "primitive equations."* The only difference is the GSM transforms these equations into spectral form. The GSM's primitive equations are based on the momentum equation, the continuity equation, and the thermodynamic equation. Winds are not actually forecast directly from the momentum equation. Instead, forecast equations for vorticity and divergence, which have been derived from the momentum equation, are used. The u- and v-component winds are derived from these forecast vorticity and divergence fields. (Sela, 1982)

In addition to the processes explicitly modeled in these equations, the GSM contains a number of other physical "parameterization" schemes.** The following paragraphs list some of the processes parameterized in the GSM.

1. Topography

The topography used in the GSM is much smoother than the earth's actual terrain. Mountain ranges appear as large domes with no jagged peaks. Fig. 5-3 shows the GSM topography over North America. The main reason for using this smooth topography is that experiments show it produces a better forecast. (Sela, 1982)

The topography appears within the primitive equations explicitly through the use of sigma coordinates. It is also used to determine surface friction effects. (Sela, 1982)

Recently, NMC has developed an improved terrain field that includes "silhouette mountains." These "silhouette mountains" still look much like those in Fig. 5-3, only they're higher. The reason for using "silhouette mountains" is to better model the blocking effects that mountains have on the winds. Depending on NMC's results, AFGWC may also switch to "silhouette mountains." (Matsumoto, 1986)

2. Surface Friction

Since the GSM includes surface friction, the winds are not necessarily geostrophic, especially near the ground. The amount of surface friction varies with the terrain. Over the Rockies and Himalayas, for

---

* For more details on the primitive equations see Haltiner and Williams (1980).

** "Parameterization: The representation, in a dynamical model, of physical effects in terms of admittedly oversimplified parameters, rather than realistically requiring such effects to be consequences of dynamics of the system. . . ." (Huschke, 1980)

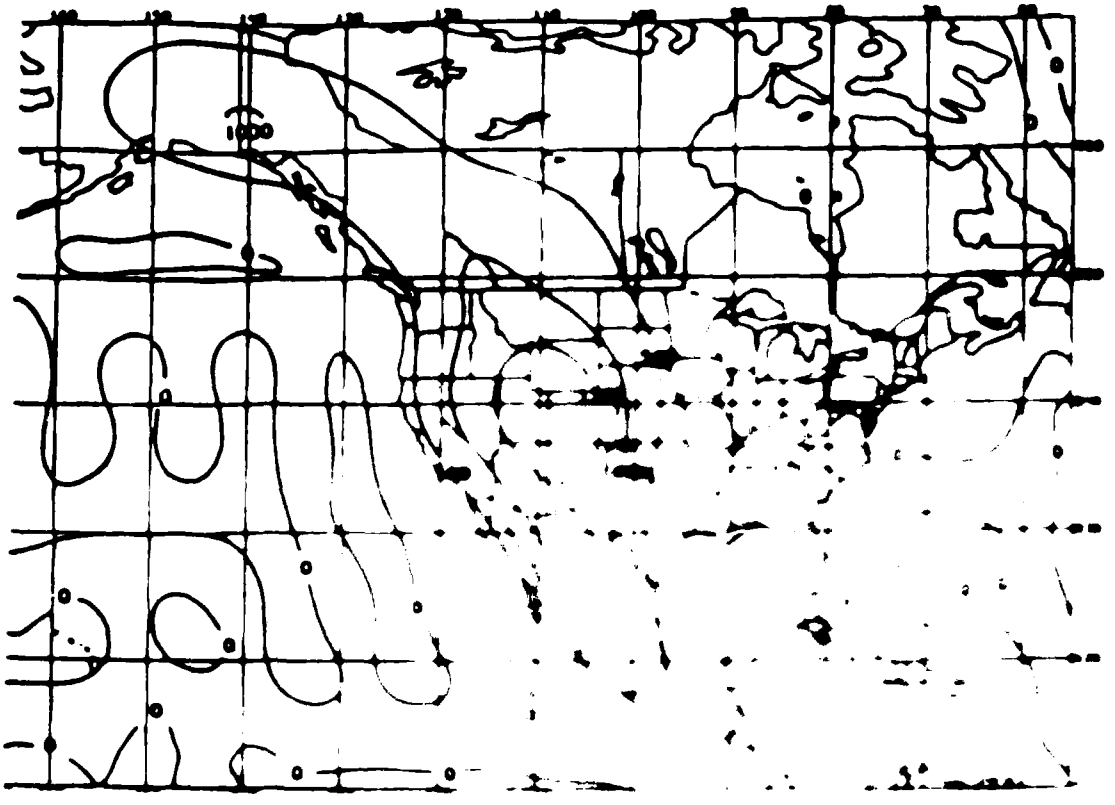

Fig. 5-3. GSM terrain heights [illegible] Weather Service, 1985b)

example, the surface friction is five times stronger than it is over the ocean. (Sela, 1982)

3. Sensible Heat Exchange

In the GSM the atmosphere can receive sensible heat only from the oceans. No heat is exchanged over land surfaces.

The scheme for receiving ocean heat uses the monthly climatology of sea surface temperatures. The amount of heat received by the atmosphere depends on the temperature difference between the water and the air, and the surface wind speed. Under windy conditions, the sensible heat exchange may be two to three times higher than it would be under calm conditions. (Sela, 1982)

4. Evaporation From the Earth's Surface

In the GSM, only moisture from the oceans may be evaporated into the atmosphere. There are no provisions for receiving moisture from the soil.

As with the sensible heat exchange, the evaporation depends on the monthly climatology of sea surface temperature and the surface wind speeds. Stronger winds result in more evaporation. (Sela, 1982)

The lack of soil moisture parameterization is a recognized weakness of the GSM. Because of this, the GSM moisture forecasts are typically too dry. The new NMC medium-range forecast model, which is also a global spectral model, does include soil moisture (National Weather Service, 1985a).

5. Precipitation Effects

Two scales of precipitation appear in the GSM. The first is the large-scale (synoptic-scale) effects. The second is the cumulus- or small-scale effects.* In both cases, when precipitation occurs, latent heat is released. Then as the precipitation falls, evaporation occurs.

Although this scheme does help the model in its moisture forecasts, the GSM is still not considered a superior precipitation forecast model. In fact, the old PE at NMC did a better job forecasting precipitation. (Sela, 1982)

6. Small-Scale Diffusion

The diffusion mechanism in the GSM is more-or-less a safety valve to keep the model stable. With all the physical parameterization schemes discussed above, the GSM would be unstable without diffusion. Basically, diffusion damps the higher frequency horizontal waves. In the operational GSM, this damping is not very severe, mainly because this GSM does not cycle back on itself. The first-guess model, however, continually cycles on itself, and thus requires much stronger diffusion. (Sela, 1982)

7. Radiation

The GSM currently does not have any radiation parameterization. There is no solar heating during the day nor radiative cooling during the night. The net result is that forecasts are typically too warm. This problem is not considered significant in the short-range forecasts (less than 3 days) from the operational GSM. The first-guess model, however, is much more vulnerable to this because of its cycling. The OI keeps this problem under control by correcting the first-guess forecast with observations every six hours. (Sela, 1982)

---

* The cumulus parameterization scheme in the GSM is known as Kuo convection (Sela, 1982); for details see Kuo (1965).

The new NMC medium-range forecast model does include radiation effects (National Weather Service, 1985a). The Air Force Geophysics Laboratory (AFGL) is investigating similar parameterizations for radiation and other physical phenomena for possible inclusion in the AFGWC GSM (Koermer, 1986).

D. Normal Modes Initialization

As we saw in Chapter 3, the GSM uses the HIRAS analysis for its initial conditions. However, before this analysis is actually used by the GSM, it undergoes a process called normal modes initialization (NMI).

The main purpose of any initialization scheme is to control mathematical instabilities that result from minor perturbations in the input data that the model can't resolve. These perturbations could be real (i.e., from micro or other sub-grid scale phenomena) or fictitious (i.e., from small observational errors, etc.). Because of this, nearly every numerical forecast model uses some form of initialization. In some of the older models, initialization would significantly alter the analysis. NMI, on the other hand, ". . .is a very gentle stroking of the data" (Sela, 1984). In fact, tests conducted by NMC indicate that NMI typically reduces the analysis wind speeds by less than 0.5 m/s (McCalla, 1985).

In spite of this small initial change, NMI has a significant effect on the final forecast, particularly in the first 24 hours. For example, Fig. 5-4 shows how NMI stabilized the surface pressure forecast in a case over the Rocky Mountains (Sela, 1982).

Finally, NMI is not absolutely necessary for the GSM. In fact, after the first 24 to 48 hours of the forecast, the GSM will take care of these instabilities on its own (Sela, 1982). The big payoff from NMI comes in reducing the error in the short-term forecasts. For this reason, both the operational GSM and the first-guess model use NMI.

E. GSM Performance Statistics and Rules of Thumb

Since its implementation in 1980, the NMC GSM has demonstrated its superiority over the old NMC PE model and the AWSPE (Matsumoto, 1985). The question is, "Just how accurate is the GSM?" To answer this question, let's look at some of the statistics NMC has compiled on the GSM since 1980.

1. Wind Verification

NMC routinely compares the GSM wind forecasts with RAOBs and aircraft data. Typically, they calculate the mean speed error (or bias) and root-mean-square (RMS) vector error. The equation for mean speed error is:

$$\text{mean speed error} = \frac{1}{N}\sum_{i=1}^{N}\left[\left(u_{fi}^2 + v_{fi}^2\right)^{1/2} - \left(u_{oi}^2 + v_{oi}^2\right)^{1/2}\right]$$

where

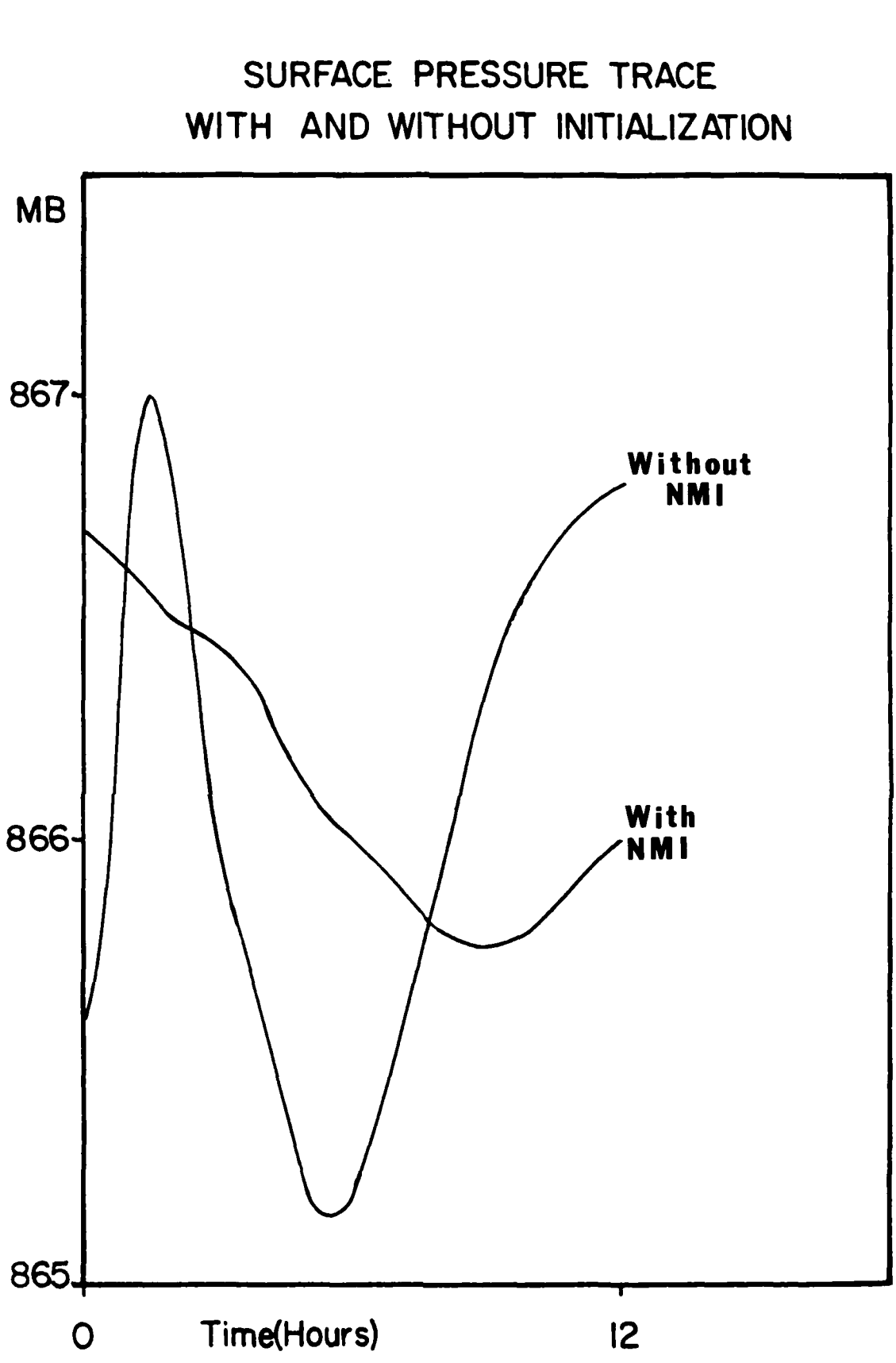

Fig. 5-4. Effect of NMI on a sample surface pressure forecast.

N = number of observations in the sample
U_{fi} = forecast u-component wind interpolated to observation point i
U_{oi} = u-component wind of observation i
V_{fi} = forecast v-component wind interpolated to observation point i
V_{oi} = v-component wind of observation i.

The equation for RMS vector error is:

$$\text{RMS vector error} = \frac{1}{N} \sum_{i=1}^{N} \left[\left(u_{fi} - u_{oi} \right)^2 + \left(v_{fi} - v_{oi} \right)^2 \right]^{1/2}$$

Fig. 5-5 shows the RMS vector errors (using northern hemisphere RAOBS) for 500 mb and 250 mb (Matsumoto, 1985). Some important aspects of these statistics include:

(1) The analysis itself has an RMS vector error of 5 m/s at 500 mb and 6 m/s at 250 mb.*

(2) The wind errors are generally less in the summer. (This is, of course, because the winds are generally lighter in the summer.)

(3) At 250 mb, the 24-hour forecast RMS vector error is usually 9 to 10 m/s.

Table 5-1 shows some results of comparing the GSM with aircraft wind observations along certain northern hemisphere air routes. These statistics are comparable to the RAOB statistics in Fig. 5-5 (McCalla, 1985).

2. Rules of Thumb

Using various NMC verification studies on the GSM, we can infer some typical performance characteristics. Below are some rules of thumb derived from these studies:

(1) The GSM does a better job of maintaining wave amplitudes than the old PE models. (Marks and Stackpole, 1983)

(2) Long waves are handled well by the GSM. This results in better long range forecasts than the old PE. (Marks and Stackpole, 1983)

(3) In winter, the GSM forecasts are much better than the old PE.

---

* Caution, this error includes both the RAOB instrument error and the analysis error. That's because this verification scheme assumes the RAOBs are exact, even though they're not. Thus, if the RAOB instrument error is 2 m/s, then even a perfect analysis would show a 2 m/s error under this verification scheme.

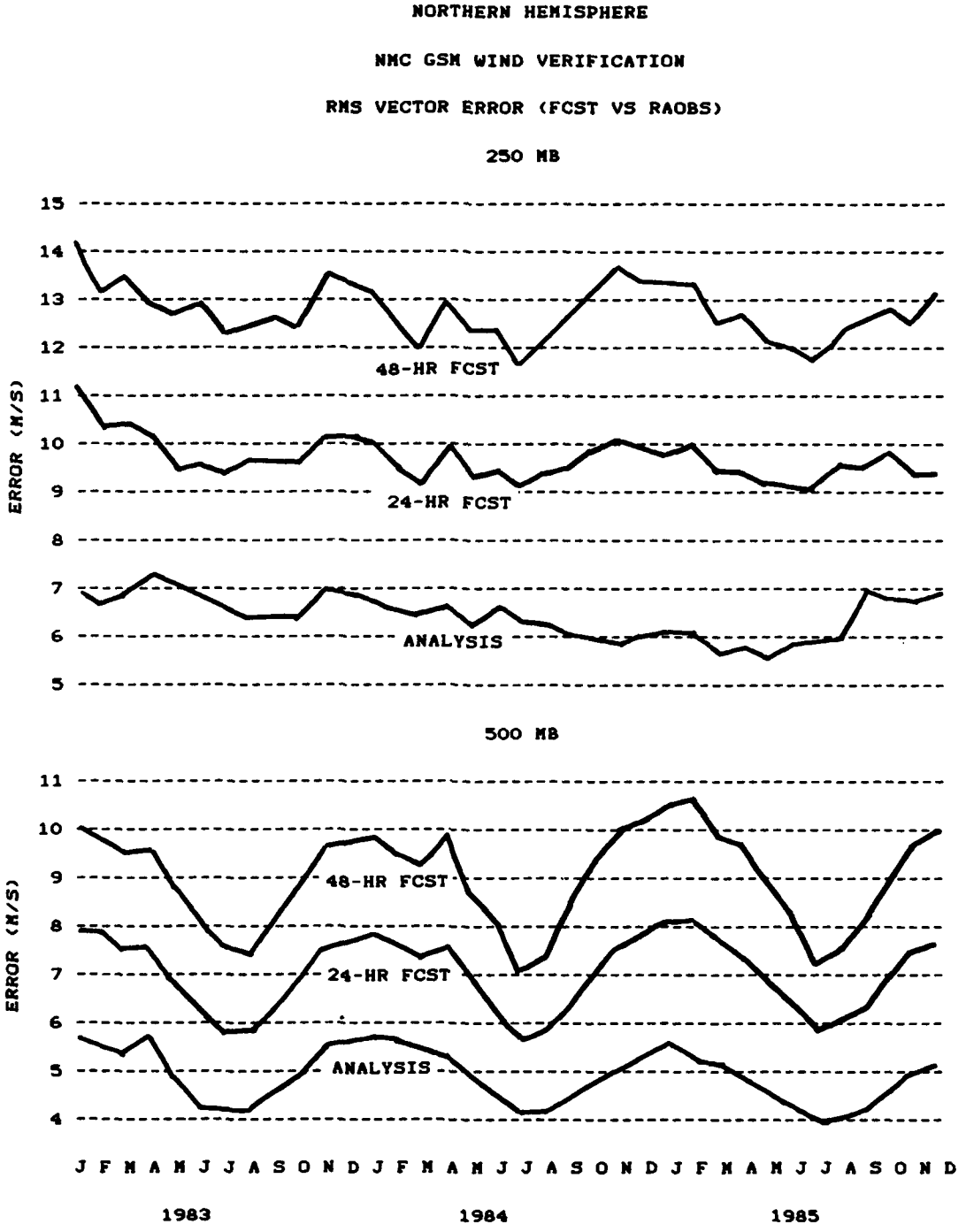

Fig. 5-5. Northern hemisphere NMC GSM wind verification statistics.

Table 5-1

GSM Forecast vs Aircraft Observations

(Winter 1984)*

	Month	Analysis	Forecast 12-HR	24-HR	36-HR	48-HR
North Pacific						
Speed Bias (m/s)	Jan	-1.6	-1.9	-2.2	-1.6	-.08
	Feb	-1.3	-2.0	-1.3	-0.7	-1.5
	Mar	-1.0	-1.4	-1.1	-1.1	-0.2
RMS Vector Error (m/s)	Jan	7.1	10.7	12.1	14.1	15.5
	Feb	6.5	10.2	11.9	12.3	13.9
	Mar	6.8	10.0	10.8	12.5	13.8
North Atlantic						
Speed Bias (m/s)	Jan	-0.5	-0.7	0.2	0.0	0.0
	Feb	-1.6	-1.1	-0.6	-0.9	-1.3
	Mar	-1.3	-1.8	-2.7	-2.6	-2.2
RMS Vector Error (m/s)	Jan	7.7	9.8	9.8	11.9	13.0
	Feb	7.6	9.8	10.6	12.2	14.4
	Mar	6.6	8.4	10.2	11.4	13.9
South Pacific						
Speed Bias (m/s)	Jan	-1.6	-2.5	-1.6	-2.7	-2.5
	Feb	-2.1	-1.8	-3.1	-3.2	-1.2
	Mar	-2.0	-0.7	-0.0	-1.3	-1.3
RMS Vector Error (m/s)	Jan	7.4	12.8	13.8	14.4	16.2
	Feb	7.3	10.3	12.4	14.2	13.8
	Mar	6.8	10.5	12.6	14.3	15.3

* From McCalla (1985)

In summer, the GSM and PE forecasts are about the same. (Marks and Stackpole, 1983)

(4) The forecast wind speeds from the GSM are typically too light in the troposphere (below 100 mb). For example, the GSM's average 48-hour, 250 mb winds are 1.5 m/s too slow. This, however, is better that the old PE, whose same forecasts were over 3 m/s too slow. (Marks and Stackpole, 1983)

(5) The GSM's 500 mb wind forecasts (24-hour and 48-hour) are more accurate than the old AWSPE by about 1 m/s. The GSM's 250 mb wind forecasts (24-hour and 48-hour) are typically 2 m/s more accurate than the old AWSPE. (Matsumoto, 1985)

(6) The GSM's wind speeds at 100 mb are generally 1 m/s too strong. (Marks and Stackpole, 1983)

(7) The GSM's temperatures at 100 mb are generally 0.7°C too cold in the winter, and 0.5°C too warm in the summer. (Marks and Stackpole, 1983)

(8) The GSM's temperature forecasts in the troposphere are generally too warm. Furthermore, since the GSM height forecasts are derived from the temperatures, the GSM forecast heights are generally too high in the troposphere. (Sela, 1982)

(9) The GSM moisture forecasts are generally too dry. Precipitation forecasts from the GSM are worse than the old NMC PE. (Sela, 1982)

F. Summary of Key Points

The GSM is primarily an aviation forecast model. Regardless of the resolution of the model itself, the display resolution is based on 30 waves (Fig. 5-1). With its vertical levels concentrated near 250 mb, the GSM's jet stream winds are about 20% better than the old AWSPE's.

The GSM contains parameterization schemes for many physical processes. Three significant exclusions, however, are radiation, sensible heat from the land, and soil moisture. These exclusions contribute to a warm bias in the troposphere and a cold bias near 100 mb. They also cause the GSM to be a bit too dry.

Overall, the GSM is a significant improvement over the AWSPE. It does a better job of maintaining wave amplitudes and wind speeds. It is particularly good at forecasting long waves.

Chapter 6 - RWM

A. General

The RWM is a limited-area, grid-point model capable of forecasting meso- and synoptic-scale weather (Mathur, 1983). It was written by NMC and transferred to AFGWC as part of the AWAPS. It can forecast for any region of the world, with a wide range of horizontal and vertical resolutions (tens of km horizontally and up to 20 vertical layers).

Its final output includes heights, winds, and temperatures at the mandatory pressure levels from 1000 mb to 50 mb. It also forecasts sea-level pressure, 1000 mb-to-500 mb thickness, 500 mb absolute vorticity, 700 mb vertical velocity, and 100 mb-to-700 mb mean relative humidity (Mathur and Facey, 1984).

Unlike the GSM, NMC has never used the RWM operationally. In fact, the testing of the RWM has been limited to individual case studies comparing it with the limited area fine mesh (LFM) model over North America and the movable fine mesh (MFM) hurricane model in the tropics. Results of these tests indicate that with similar resolutions, the RWM forecasts are comparable to both the LFM and MFM (Mathur, 1983).

For the remainder of this chapter, let's look at some of the basic concepts behind the RWM and see what physical process it includes. For a more detailed description of the model, including equations, see Mathur (1983).

B. A Quasi-Lagrangian Model

The RWM is referred to as a quasi-Lagrangian model. You might ask, "What's a 'quasi-Lagrangian'?" First, Lagrangian is a term used to describe a type of coordinate system. Using Lagrangian coordinates, you can examine how an air parcel's properties change by "following along" with the parcel as it moves. The alternative is to examine the air parcel at a fixed time over a fixed location (such as a set of grid points)--this is done using Eulerian coordinates. Weather maps use Eulerian coordinates while trajectory bulletins use Lagrangian coordinates.

The RWM uses a combination of these two coordinate systems. In the Eulerian sense, it still produces forecasts for fixed grid points. However, predictions are carried out following individual parcels. Specifically, the RWM accounts for changes in parcel accelerations and follows each parcel along its trajectory. By using this scheme, the RWM's is expected to do particularly well in forecasting jet streams and rapidly developing storm systems.

C. Physical Parameterization

The RWM contains essentially the same physical parameterizations as the GSM. Through the use of sigma coordinates, it compensates for surface elevation. It also varies frictional effects according to the terrain height. It allows for sensible heat exchange and surface moisture evaporation over the oceans. It models large-scale moisture processes (condensation, precipitation, and evaporation) and cumulus-scale moisture processes (using Kuo-type convection). Like the GSM, it uses horizontal diffusion to control noise and currently does not include any radiation effects.

Since the RWM is not a global model, it must also have horizontal boundary conditions. Presently, it is configured to use the GSM forecast (valid every six hours) for this purpose.

D. Summary of Key Points

Since the RWM has no operational history, I cannot offer any "rules of thumb" for using it. One important point to keep in mind, however, is the resolution of the particular forecast. Do not expect the RWM to forecast mesoscale features smaller than the model's resolution. Furthermore, if the RWM uses the HIRAS as its initial conditions, its starting resolution will be that of the HIRAS.

Chapter 7 - Summary

In this report we've tried to take a forecaster's view of the AWAPS. We began with some basic NWP, just to make sure we knew the difference between an analysis and a forecast model and the difference between a grid-point model and a spectral model. Then we looked at the AWAPS production cycle and how the HIRAS, GSM, and RWM all fit together.

Next, we looked at each model separately. First, we saw how the HIRAS uses optimum interpolation to combine a first guess and observations into a final analysis. We saw how HIRAS considers the various instrument types and the accuracy of the first guess to do its analysis. We also saw how the surface, tropospheric, and stratospheric analyses each have their own special considerations. Then we took a close-up look at the analysis cycle and how manual and automated data QC are done.

In the next chapter we looked at the GSM. We first tried to see what a 30-wave resolution model looks like on a grid-point map. Next we saw how the 12 vertical layers in the GSM are clustered around 250 mb to improve jet stream forecasts. We also looked at the various parameterization schemes included in the GSM. Finally we looked at some NMC verification statistics on the GSM and some rules of thumb developed by National Weather Service over the past five years.

In Chapter 6 we took a very quick look at the RWM. We saw that it is a quasi-Lagrangian grid-point model that includes most of the same physical parameterization schemes present in the GSM. Although the RWM has no operational history, we expect it to improve mesoscale and synoptic scale forecasts over limited regions, particularly in rapidly developing systems.

In conclusion, this report is meant to get you started on the right track with AWAPS. Hopefully, now you can use the AWAPS with confidence, and when the situation warrants, modify its guidance to produce an even better forecast.

REFERENCES

Carr, E.L. and J.P. Tuell, 1985: Optimum interpolation technique applied to a stratosphere analysis. Preprints Seventh Conference on Numerical Weather Prediction, Montreal, P.Q., Canada, Amer. Meteor. Soc., 54-56.

Dey, C.H. and L.L. Morone, 1985: Evolution of the National Meteorological Center global data assimilation system: January 1982 - December 1983. Mon. Wea. Rev., 113, 304-318.

Haltiner, G.J. and R.T. Williams, 1980: Numerical Prediction and Dynamic Meteorology, John Wiley & Sons, New York, 477 pp.

High Resolution Analysis System Users Manual, 1985: Air Force Global Weather Central, Offutt AFB, Ne.

Hughes, W.L., 1981: Numerical forecasts of tropopause and maxwind. Proc. Second Meeting of the International Civil Aviation Organization Area Forecast Panel, Montreal, P.Q., Canada.

Huschke, R.E. (editor), 1980: Glossary of Meteorology, Amer. Meteor. Soc., Boston, Ma., 638 pp.

Koermer, J.P., 1986: Personal Communications.

Kuo, H.L., 1965: On formation and intensification of tropical cyclones through latent heat release by cumulus convection. J. Atmos. Sci., 22, 40-63.

Kurihara, Y. and J. Holloway, 1967: Numerical integration of a nine level global primitive equation model formulated buy the box method, Mon. Wea. Rev., 95, 509-530.

Marks, D.G. and J.D. Stackpole, 1983: Some performance comparisons between NMC's spectral model and the seven-layer primitive equation model, NMC Office Note 277, U.S. Department of Commerce, NOAA, NWS, Washington, DC.

Mathur, M.B., 1983: A quasi-Lagrangian regional model designed for operational weather prediction. Mon. Wea. Rev., 111, 2087-2098.

____, and W.B. Facey Jr., 1984: Relocatable window model maintenance manual. Unpublished manual, Air Force Global Weather Central, Offutt AFB, Ne.

____, and ____, 1984: Relocatable window model users manual. Unpublished manual, Air Force Global Weather Central, Offutt AFB, Ne.

Matsumoto, C.R., 1985: Model performance statistics from AFGWC, FNOC, and NMC. Unpublished graphs, Headquarters Air Weather Service, Scott AFB, Il.

____, 1986: Personal Communications.

McCalla, M.R.P., 1985: Verfication of NMC's spectral model jet-level oceanic winter season forecasts by use of aircraft data. Mon. Wea. Rev., 113, 684-691.

McPherson, D.D., 1980: Evolution and present status of objective analysis/assimilation at NMC, NMC Office Note 216, U.S. Department of Commerce, NOAA, NWS, Washington, DC.

____, 1982: Optimum interpolation: basic formulation and characteristics, NMC Office Note 265, U.S. Department of Commerce, NOAA, NWS, Washington, DC.

Nastrom, G.D., 1985: NWP models at a glance, AWS/FM-85-007, Headquarters Air Weather Service, Scott AFB, Il.

National Weather Service, 1983: Some performance cmparisons between the spectral and seven-layer PE models, Western Region Technical Attachment No. 83-17, U.S. Department of Commerce, NOAA, NWS, Washington, DC.

National Weather Service, 1985: New medium range forecast model, Technical Procedures Bulletin No. 349, U.S. Department of Commerce, NOAA, NWS, Washington, D.C.

National Weather Service, 1985: NMC model terrain, Western Region Technical Attachment No. 85-28, U.S. Department of Commerce, NOAA, NWS Washington, DC.

Phillips, N.A., 1959: Numerical integration of the primitive equations on the hemisphere. Mon. Wea. Rev., 87, 333-345.

Sela, J.G., 1982: The NMC spectral model, NOAA Technical Report NWS 30, U.S. Department of Commerce, NOAA, NWS, Washington, D.C.

____, 1984: Tape recording of training on global spectral model, conducted May 1984, at National Meteorological Center, Washington, D.C.

Stobie, J.G., M.D. Lewis, M.A. Langford, J.P. Tuell, and E.L. Carr, 1985: The use of optimum interpolation at AFGWC. Preprints Seventh Conference on Numerical Weather Prediction, Montreal, P.Q., Canada, Amer. Meteor. Soc., 43-49.

Warburton, J., 1982: Personal communications.

____, and Sela, J.G., 1984: The global spectral model maintenance manual. Unpublished manual, Air Force Global Weather Central, Offutt AFB, Ne.

____, and ____, 1984: The global spectral model users manual. Unpublished manual, Air Force Global Weather Central, Offutt AFB, Ne.

Wilfong, T.L., 1985: Air Force Global Weather Central's advanced weather analysis and prediction system. Preprints Seventh Conference on Numerical Weather Prediction, Montreal, P.Q., Canada, Amer. Meteor. Soc., 452-454.

____, J.G. Stobie, M.D. Lewis, J.P. Tuell, and E.L. Carr, 1985: Advanced weather analysis and prediction (AWAPS) global spectral model (GSM) database specifications. Unpublished manual, Air Force Global Weather Central, Offutt AFB, Ne.

Appendix A

MECHANICS OF OPTIMUM INTERPOLATION

To understand the mechanics of optimum interpolation (OI), consider a simple analysis using three observations (Fig. A-1) . To make this analysis as simple as possible, make the following assumptions:

1. All three observations are at the same pressure level as the grid point (vertical correlation = 1).
2. All the observing instruments are perfect (no instrument errors).
3. The first guess is totally unreliable compared to the observations (draw for the observations).
4. All the observations are unique (no redundant observations from the same instrument).
5. Analyze heights using only height observations (univariate).

The first step is to calculate the residuals between the observations and the first guess using

Residual = Observation - First Guess.

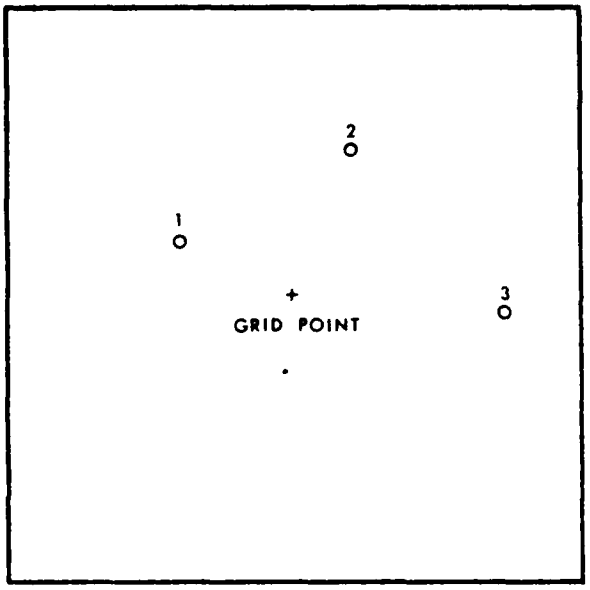

Fig. A-1. Array of three observations surrounding an analysis grid point.

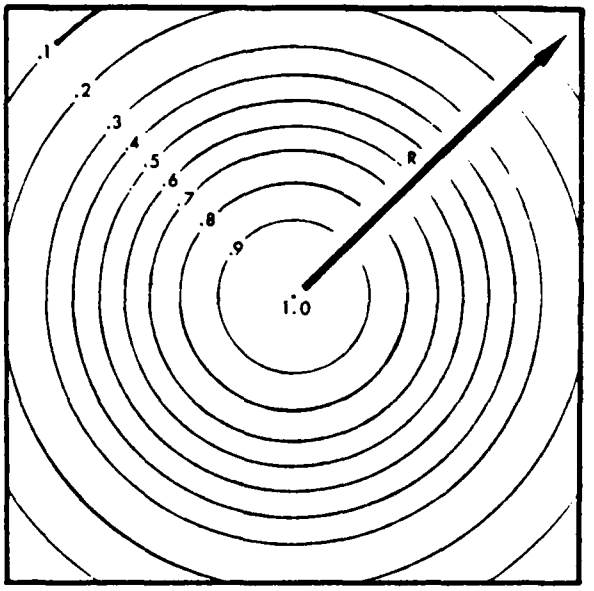

Fig. A-2. Graphical representation of horizontal correlation function (1).

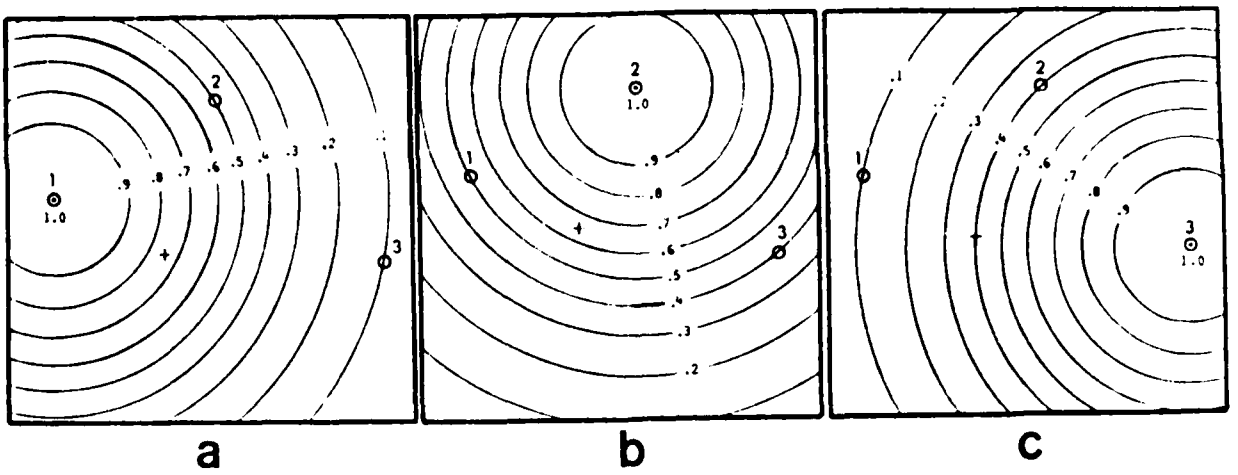

Fig. A-3. Horizontal correlation function centered at (a) observation #1, (b) observation #2, and (c) observation #3.

Next, calculate correlations between the observations and the grid point. At NMC and AFGWC the horizontal correlation is modeled by*

$$HCOR = EXP(-CH*(R**2)) \quad (1)$$

where: HCOR = horizontal correlation
CH = a positive constant
R = horizontal distance between points.

This function is shown graphically in Fig. A-2. Next, use these correlations to develop a series of linearly independent equations. Specifically, overlay Fig. A-2 onto Fig. A-1 as shown in Fig. A-3a. The following equation results:

$$1.0*W(1) + 0.5*W(2) + 0.1*W(3) = 0.75 \quad (2)$$

where: W(1) = weight to be assigned to observation #1
W(2) = weight to be assigned to observation #2
W(3) = weight to be assigned to observation #3.

In eqn (2), 1.0 is the correlation between observation #1 and itself, 0.5 is the correlation between observation #1 and observation #2, 0.1 is the correlation between observation #1 and observation #3, and 0.75 is the correlation between observation #1 and the analysis grid point. The second equation results by moving the center of Fig. A-2 to observation #2 (Fig. A-3b):

$$0.5*W(1) + 1.0*W(2) + 0.4*W(3) = 0.65 \quad (3)$$

---

* With the exception of equations (2), (3), (4), and (7); equations in this appendix appear in standard FORTRAN notation.

The third equation results by moving the center of Fig. A-2 to observation #3 (Fig. A-3c):

$$0.1*W(1) + 0.4*W(2) + 1.0*W(3) = 0.4 \quad (4)$$

Now solve eqns (2), (3) and (4) for the three unknowns W(1), W(2), and W(3). Then obtain the analysis residual at the grid point by

$$\text{Analysis Residual} = W(1)*(OBRES(1)) + W(2)*(OBRES(2)) + W(3)*(OBRES(3))$$

where: OBRES(I) = residual for observation I.

Finally, calculate the net analysis at the grid point using

Net Analysis = Analysis Residual + First Guess.

In this simple example we used only the horizontal distance to determine the weights assigned to each observation. In practice, the NMC and AFGWC OI models also consider:

1. Vertical distance
2. Instrument quality
3. Quality of the first guess
4. Redundancy of observations.

The vertical distance is accounted for by using the following vertical correlation function:

$$VCOR = 1/(1+CP*(LOG(P(1)/P(2)))**2) \quad (5)$$

where: VCOR = vertical correlation
CP = positive constant
P(1) = pressure at point #1
P(2) = pressure at point #2

and combining the vertical and horizontal correlations into a total correlation

$$TCOR = HCOR * VCOR. \quad (6)$$

TCOR is then used in place of HCOR to produce the series of linear equations.

To see how to adjust for the instrument errors and the quality of the first guess, examine eqns (2), (3), and (4) in matrix form

$$\begin{pmatrix} 1.0 & 0.5 & 0.1 \\ 0.5 & 1.0 & 0.4 \\ 0.1 & 0.4 & 1.0 \end{pmatrix} \begin{pmatrix} W(1) \\ W(2) \\ W(3) \end{pmatrix} = \begin{pmatrix} .75 \\ .65 \\ .40 \end{pmatrix}$$

or $\underline{A}\,\underline{W} = \underline{B}$ (7)

Notice that $\underline{A}$ will always be symmetric with the diagonal terms equal to 1.0. To compensate for instrument errors and the quality of the first guess, the diagonal terms in $\underline{A}$ are modified using

$$A(I,I) = 1+((OBER)/(FGER))^{**}2 \qquad (8)$$

where: A(I,I) = diagonal term in $\underline{A}$ for observation I
OBER = expected error of the instrument used for observation I
FGER = expected forecast error (based on quality of previous analyses).

Three types of observation redundancies are compensated for in the NMC and AFGWC OI models. These include (1) observations taken at different vertical levels by the same RAOB, (2) observations taken at different vertical levels by the same satellite, and (3) observations taken at different horizontal locations by the same satellite. In cases (1) and (2) an interobservational error correlation similar to VCOR is used. For case (3), an interobservational error correlation similar to HCOR is used. At NMC these interobservational error correlations are introduced using the following equation:

$$A(I,J) = TCOR(I,J) + ERCOR*(OBER(I)/FGER(I))*(OBER(J)/FGER(J)) \qquad (9)$$

where: A(I,J) = final correlation between observations I and J
TCOR(I,J) = result of eqn (6) for observations I and J
ERCOR = interobservational error correlation between observation I and J
OBER(I) = expected error of the instrument used for observation I
OBER(J) = expected error of the instrument used for observation J
FGER(I) = expected forecast error at observation location I (based on quality of previous analyses)
FGER(J) = expected forecast error at observation location J (based on quality of previous analyses).

Finally, the OI models at both NMC and AFGWC are multivariate. That is, height and wind observations are used in the height anlayses and in the wind analyses. This is accomplished by applying the geostrophic wind relationships to the horizontal correlations (except near the equator where the analysis remains univariate).

Appendix B

HIRAS Analysis Fields

Table B-1 shows the analysis fields produced by HIRAS on the 2.5 X 2.5 degree latitude-longitude grid. The HIRAS directly analyzes the heights, temperature, u-component wind, v-component wind, and specific humidity. All the other fields listed in Table B-1 are derived from these five basic fields. Here is a short description of how AWAPS calculates these remaining fields.

1. Sea Level Pressure

The sea level pressure is derived from the 1000 mb height and temperature using the hypsometric equation. The AWAPS equation is:

$$P_{sl} = (P_{std})\, e^{gh/RT} \qquad (1)$$

where

P_{sl} = sea level pressure
P_{std} = globally averaged sea level pressure
g = acceleration of gravity
h = D-value of 1000 mb surface
R = gas constant for dry air
T = temperature at 1000 mb.

2. Temperature Advection

This field is calculated using the temperatures and winds. Fig. B-1 shows a typical grid used for this calculation. Using Fig. B-1, the AWAPS equation for this field is:

$$T_{adv} = \left(\frac{T_2 - T_1}{dx}\right) u_o + \left(\frac{T_4 - T_3}{dy}\right) v_o \qquad (2)$$

where

T_{adv} = temperature advection
T_i = temperature at grid point i
dx = distance between grid points 1 and 2
dy = distance between grid points 3 and 4
u_o = u-component wind at grid point o
v_o = v-component wind at grid point o.

TABLE B-1

HIRAS ANALYSIS FIELDS

Field	Pressure Levels																Layers						
	SURFACE	1000 mb	850 mb	700 mb	500 mb	400 mb	300 mb	250 mb	200 mb	150 mb	100 mb	70 mb	50 mb	30 mb	20 mb	10 mb	SFC-850 mb	850-700 mb	700-500 mb	500-400 mb	400-300 mb	300-100 mb	Tropopause
Sea-Level Pressure	X																						
Heights (D-value)		X	X	X	X	X	X	X	X	X	X	X	X	X	X	X							
Temperature	X	X	X	X	X	X	X	X	X	X	X	X	X	X	X	X							
Temperature Advection																	X						
U-component wind	X	X	X	X	X	X	X	X	X	X	X	X	X	X	X	X							
V-component wind	X	X	X	X	X	X	X	X	X	X	X	X	X	X	X	X							
Relative Humidity	X	X	X	X	X	X	X																
Specific Humidity	X	X	X	X	X	X	X																
Dewpoint Depression	X	X	X	X	X	X	X																
Precipitable Water																	X	X	X	X	X	X	
Vorticity			X		X		X																
Vorticity Advection			X		X																		
Stream Function	X	X	X	X	X	X	X	X	X	X	X	X	X	X	X	X							
Tropopause pressure																							X
Tropopause temperature																							X
Tropopause height																							X

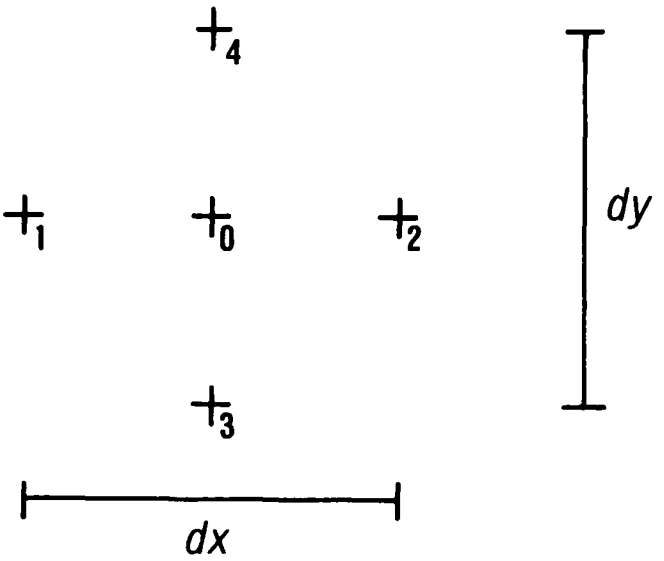

Fig. B-1. Typical array of HIRAS grid points.

The temperature advection for the layer SFC - 850 mb is the arithmetic average of T_{adv} at 1000 mb and 850 mb. That is:

$$T_{adv_{(Sfc-850)}} = \frac{T_{adv_{(1000)}} + T_{adv_{(850)}}}{2} \tag{3}$$

3. Relative Humidity

Relative humidity is derived from the pressure, specific humidity, and the temperature. The equation in AWAPS is:

$$RH = \frac{e_q}{e_s} \tag{4}$$

where

RH = relative humidity
e_q = vapor pressure (calculated from q)
e_s = saturation vapor pressure (calculated from T).

The saturation vapor pressure is derived from the temperature, T, using a sixth order polynomial that approximates the Clausius-Clapeyron equation. This equation is:

$$e_s = 6984.505294 - 188.9039310\ T + 2.133357675\ T^2 - (1.288580973 \times 10^{-2})\ T^3 + (4.393587233 \times 10^{-5})\ T^4 - (8.023923082 \times 10^{-8})\ T^5 + (6.136820929 \times 10^{-11})\ T^6 \tag{5}$$

This equation is accurate to within 1% over the temperature range -50 C to +50 C. Outside this temperature range AWAPS uses the Clausius Clapeyron equation directly, which is:

$$e_s = 6.11\ e^{\left[\frac{L_v}{R_v}\left(\frac{1}{273.16} - \frac{1}{T}\right)\right]} \tag{6}$$

where

$L_v = (2.5X10^6 - 2274(T-273.16))$

and

L_v = latent heat of vaporization
R_v = gas constant for water vapor.

The vapor pressure of the air is calculated using the following equation:

$$e_q = \frac{P\,q}{.622 + (1-.622)q} \tag{7}$$

where

P = pressure
q = specific humidity.

4. Dewpoint Depression

The dewpoint depression is calculated from the pressure, temperature, and specific humidity using the Clausius-Clapeyron equation. The AWAPS equation is:

$$T_d = \frac{1}{\left[\left(\frac{1}{273.16}\right) - \left(\frac{R_v}{L_v}\right) ln\left(\frac{e_q}{e_o}\right)\right]} \tag{8}$$

where

T_d = dewpoint
R_v = gas constant for water vapor
L_v = latent heat of vaporization (see RH calculation)
e_q = vapor pressure (see RH calculation)
e_o = saturation vapor pressure at 0 C.

5. Precipitable Water

The precipitable water is calcualted from the specific humidity and the depth of the layer:

$$PW = \left(\frac{q_1 + q_2}{2}\right)\left(\frac{P_2 - P_1}{g}\right)k \tag{9}$$

where

PW = precipitable water
P_1 = pressure of the upper boundary of the layer
P_2 = pressure of the lower boundary of the layer
q_1 = specific humidity at the upper boundary of the layer
q_2 = specific humidity at the lower boundary of the layer
g = acceleration of gravity
k = constant to give result in mm (if pressure is in mb and g is in m/s, then k = 10).

In the topmost layer (300-100 mb), the 100 mb specific humidity is derived from climatology based on the temperature. All the other specific humidities come directly from the HIRAS analysis.

6. Vorticity

In the mid-latitudes the vorticity is calculated using the heights. That is, it is the geostrophic vorticity, which uses the Laplacian of the heights. Using Fig. B-1, the mid-latitude equation for vorticity is:

$$\zeta = f + \frac{g}{f}\left[\frac{Z_1 + Z_2 + Z_3 + Z_4 - 4Z_0}{\left(\frac{dx + dy}{2}\right)^2}\right] \qquad (10)$$

where

ζ = vorticity
f = coriolis parameter
g = acceleration of gravity
Z_i = height at grid point i
dx = distance between grid points 1 and 2
dy = distance between grid points 3 and 4.

In the tropics, the vorticity is calculated using the winds. This equation uses the curl of the wind field. Using Fig. B-1, the AWAPS equation is:

$$\zeta = f + \left(\frac{v_2 - v_1}{dx} - \frac{u_4 - u_3}{dy}\right) \qquad (11)$$

where

u_i = u-component wind at grid point i
v_i = v-component wind at grid point i.

These two fields are both smoothed and then blended together in the subtropics.

7. Vorticity Advection

The vorticity advection is calculated using the vorticity and the winds. The AWAPS equation is:

$$\zeta_{adv} = \left(\frac{\zeta_2 - \zeta_1}{dx}\right) u_o + \left(\frac{\zeta_4 - \zeta_3}{dy}\right) v_o \qquad (12)$$

where

ζ_{adv} = vorticity advection
ζ_i = vorticity at grid point i
dx = distance between grid points 1 and 2 (Fig. B-1)
dy = distance between grid points 3 and 4 (Fig. B-1)
u_o = u-component wind at grid point o
v_o = v-component wind at grid point o.

8. Stream Function

The stream function is calculated using the height field. The equation AWAPS uses is:

$$\psi = \frac{g Z}{f} \qquad (13)$$

where

ψ = stream function
g = acceleration of gravity
f = coriolis parameter at 45 degrees latitude
Z = height.

9. Tropopause Variables

The tropopause level is calculated using an algorithm that uses the WMO definition of the tropopause. For more on this method see Hughes (1981). Incidently, in this algorithm the tropopause is not allowed to be outside the range of 450 mb to 85 mb.

Appendix C

GSM Forecast Fields

Table C-1 shows the forecast fields that the GSM creates on the 2.5 X 2.5 degree latitude-longitude grid. The primary forecast fields used by the model are temperature, divergence, vorticity, and specific humidity. From these fields the GSM calculates and outputs sea level pressure, heights, temperature, u-component wind, v-component wind, vertical velocity, specific humidity, 500 mb vorticity, and all the tropopause data. The remaining fields in table C-1 are derived from these fields using the techniques described in Appendix B.

Table C-2 shows the forecast intervals for each field output by the GSM. You'll notice that this table does not include moisture. That's because AFGWC is still evaluating the GSM's moisture forecasting capability. In the mean time, all AFGWC moisture forecasts still come from the cloud forecast model commonly referred to as the "five-layer model."

TABLE C-1

GSM FORECAST FIELDS

Field	Pressure Levels												
	SURFACE	Gradient Level	1000 mb	850 mb	700 mb	500 mb	400 mb	300 mb	250 mb	200 mb	150 mb	100 mb	1000-850 mb	Tropopause
Sea-Level Pressure	X													
Heights (D-value)			X	X	X	X	X	X	X	X	X	X		
Temperature	X		X	X	X	X	X	X	X	X	X	X		
Temperature Advection													X	
U-component wind		X	X	X	X	X	X	X	X	X	X	X		
V-component wind		X	X	X	X	X	X	X	X	X	X	X		
Vertical Velocity			X	X	X	X	X	X	X	X	X			
Relative Humidity			X	X	X	X	X							
Specific Humidity	X		X	X	X	X	X							
Dewpoint Depression			X	X	X	X	X							
Vorticity				X		X		X						
Vorticity Advection						X								
Stream Function			X	X	X	X	X	X	X	X	X	X		
Tropopause pressure														X
Tropopause temperature														X
Tropopause height														X

TABLE C-2

GSM FORECAST INTERVALS

Field	Forecast Interval (hours)																					
	00	03	06	09	12	15	18	21	24	27	30	33	36	42	45	48	51	54	57	60	72	96
Sea-Level Pressure	X	X	X	X	X	X	X	X	X	X	X	X	X									
Heights (D-value)	X	X	X	X	X	X	X	X	X	X	X	X	X	X	X	X	X	X	X	X	X	*
Temperature	X	X	X	X	X	X	X	X	X	X	X	X	X	X	X	X	X	X	X	X	X	*
Temperature Advection	X	X	X	X	X	X	X	X	X													
U-component Wind	X	X	X	X	X	X	X	X	X	X	X	X	X	X	X	X	X	X	X	X	X	
V-component Wind	X	X	X	X	X	X	X	X	X	X	X	X	X	X	X	X	X	X	X	X	X	
Vertical Velocity	X	X	X	X	X	X	X	X	X	X	X	X	X	X	X	X	X	X	X	X		
Vorticity	X	X	X	X	X	X	X	X	X	X	X	X	X	X	X	X	X	X	X	X		
Vorticity Advection	X	X	X	X	X	X	X	X	X	X	X	X	X									
Stream Function	X	X	X	X	X	X	X	X	X	X	X	X	X	X	X	X						
Tropopause pressure	X	X	X	X	X	X	X	X	X	X	X	X	X	X	X	X						
Tropopause temperature	X	X	X	X	X	X	X	X	X	X	X	X	X	X	X	X	X	X	X	X	X	
Tropopause height	X	X	X	X	X	X	X	X	X	X	X	X	X	X	X	X	X	X	X	X	X	

* 96-hour forecast contains only 1000 mb and 500 mb D-values and temperatures.

DISTRIBUTION

AWS/DNT, Scott AFB, IL 62225-5008.....3
AWS/DNX, Scott AFB, IL 62225-5008.....1
AWS/DO, Scott AFB, IL 62225-5008.....1
AWS/SY, Scott AFB, IL 62225-5008.....1
Aerospace Data Fac (OL A), Buckley ANG Base, Aurora, CO 80011-9599.....1
OL-B, HQ AWS, Langley AFB, VA 23665-5000.....1
OL-C, HQ AWS, Chanute AFB, IL 61868-5000.....5
OL-E, HQ AWS, ATZL-CAW-E, Ft Leavenworth, KS 66027-5300.....1
SD/YDA, PO Box 92960, Worldway Postal Ctr, Los Angeles, CA 90009-2960.....1
OL-G, HQ AWS, NHC Rm 631, 1320 S Dixie Hwy, Coral Gables, FL 33146-2976...1
OL-H, HQ AWS (ATSI-CD-SWO), Ft Huachuca, AZ 85613-5000.....1
AFOTEK OL-NX, 1313 Halley Circle, Norman, OK 73069-8476.....1
OL-I, HQ AWS (ATDO-WE), Ft Monroe, VA 23651-5000.....1
Det 1, HQ AWS, Pentagon, Washington, DC 20330-6560.....1
Det 2, HQ AWS, Washington, DC 20330-5054.....2
AFSCF/WE, PO Box 3430, Sunnyvale AFS, CA 94088.....1
Det 8, HQ AWS, PO Box 4239N, Las Vegas, NV 89030.....1
Det 9, HQ AWS, PO Box 12297, Las Vegas, NV 89112-0297.....1
1WW/DN, Hickam AFB, HI 96853-5000.....7
20WS/DN, APO San Francisco 96328-5000.....12
30WS/DN, APO San Francisco 96301-0420.....16
2WW/DN, APO New York 09012-5000.....7
7WS/DN, APO New York 09403-5000.....30
28WS/DN, APO New York 09127-5000.....10
31WS/DN, APO New York 09223-5000.....20
3WW/DN, Offutt AFB, NE 68113-5000.....3
9WS/DN, March AFB, CA 92518-5000.....15
11WS/DN, Elmendorf AFB, AK 99506-5000.....11
24WS/DN, Randolph AFB, TX 78150-5000.....12
26WS/DN, Barksdale AFB, LA 71110-5002.....21
4WW/DN, Peterson AFB, CO 80914-5000.....12
2WS/DN, Andrews AFB, MD 20334-5000.....19
5WW/DN, Langley AFB, VA 23665-5000.....8
1WS, MacDill AFB, FL 33608-5000.....2
3WS/DN, Shaw AFB, SC 29152-5000.....13
5WS/DN, Ft McPherson, GA 30330-5000.....26
25WS/DN, Bergstrom AFB, TX 78743-5000.....13
AFGWC/DO, Offutt AFB, NE 68113-5000.....1
AFGWC/SD, Offutt AFB, NE 68113-5000.....100
AFGWC/SDSL, Offutt AFB, NE 68113-5000.....5
7WW/DN, Scott AFB, IL 62225-5008.....7
6WS, Hurlburt Fld, FL 32544-5000.....1
15WS/DN, McGuire AFB, NJ 08641-5002.....12
17WS/DN, Travis AFB, CA 94535-5000.....16
3350 TECH TG/TTGU-W, Stop 62, Chanute AFB, IL 61868-5000.....5
AUL/LSE, Maxwell AFB, AL 36112-5564.....1
Naval Research Laboratory, Code 4323, Washington, DC 20375.....1
NAVOCEANCOMFAC, NSTL, Bay St Louis, MS 39529-5002.....1
COMNAVOCEAN, NSTL, Bay St Louis, MS 39529-5000.....1
NAVOCEANO, ATTN Code 9220 (Tony Ortolano), Bay St Louis, MS 39522-5001....2

NEPRF, Monterey, CA 93943-5106.....1
Naval Post-Graduate School, NC4(63rd), Monterey, CA 93943-5100.....1
NWS/SR, Scientific Services Division W/SR 3X3, 819 Taylor St, Rm 10A26
Fort Worth, TX 76102.....1
U.S. Army Atmospheric Sciences Laboratory, White Sands Missile Range, NM
88002-5000.....1
AFGL/LY, Hanscom AFB, MA 10731-5000.....2
AFCSA/SAGW, Washington, DC 20330-5420.....5
Technical Library, Dugway Proving Ground, Dugway, UT 84022-5000.....1
AWSTL, Scott AFB, IL 62225-5458.....100

END

11-86

DTIC